

Black Holes in Higher-Dimensional Gravity

Niels A. Obers

The Niels Bohr Institute

Blegdamsvej 17, 2100 Copenhagen , Denmark

obers@nbi.dk

Abstract

These lectures review some of the recent progress in uncovering the phase structure of black hole solutions in higher-dimensional vacuum Einstein gravity. The two classes on which we focus are Kaluza-Klein black holes, i.e.: static solutions with an event horizon in asymptotically flat spaces with compact directions, and stationary solutions with an event horizon in asymptotically flat space. Highlights include the recently constructed multi-black hole configurations on the cylinder and thin rotating black rings in dimensions higher than five. The phase diagram that is emerging for each of the two classes will be discussed, including an intriguing connection that relates the phase structure of Kaluza-Klein black holes with that of asymptotically flat rotating black holes.

Contents

1	Introduction and motivation	1
2	Uniqueness theorems and going beyond four dimensions	5
2.1	Black hole (non-)uniqueness	5
2.2	Overview of solution methods	7
3	Kaluza-Klein black holes	8
3.1	Setup and physical quantities	9
3.2	Black holes and strings on cylinders	10
3.3	Phase diagram and copied phases	14
3.4	KK phases on T^2 from phases on S^1	16
4	Multi-black hole configurations on the cylinder	18
4.1	Construction of multi-black hole solutions	18
4.2	Newtonian derivation of the thermodynamics	21
4.3	Consequences for the phase diagram	23
5	Thin black rings in higher dimensions	25
5.1	Thin black rings from boosted black strings	25
5.2	Matched asymptotic expansion	28
5.3	Black rings versus MP black holes	30
6	Completing the phase diagram	33
6.1	GL instability of ultra-spinning MP black hole	33
6.2	Phase diagram of neutral rotating black holes on M^D	35
7	Outlook	37
	References	40

1 Introduction and motivation

The study of the phase structure of black objects in higher-dimensional gravity (see e.g. the reviews [1, 2, 3, 4]) is interesting for a wide variety of reasons. First of all, it is of intrinsic interest in gravity where the spacetime dimension can be viewed as a tunable parameter. In this way one may discover which properties of black holes are universal and which ones show a dependence on the dimension. We know for example that the laws of black hole mechanics are of the former type, while, as will be illustrated in this lecture, properties such as uniqueness and horizon topology are of the latter type. In particular, recent research has revealed that as the dimension increases the phase structure becomes increasingly intricate and diverse. In this context, another interesting phenomenon that

has been observed is the existence of critical dimensions, above which certain properties of black holes can change drastically. Uncovering the phases of black holes is also relevant for the issue of classical stability of black hole solutions as well as gravitational phase transitions between different solutions, such as those that involve a change of topology of the event horizon. Furthermore, information about the full structure of the static or stationary phases of the theory can provide important clues about the time-dependent trajectories that interpolate between different phases.

Going beyond pure Einstein gravity, there are also important motivations originating from String Theory. String/M-Theory at low energies is described by higher-dimensional theories of gravity, namely various types of supergravities. As a consequence, black objects in pure gravity are often intimately related to black hole/brane solutions in string theory. These charged cousins and their near-extremal limits play an important role in the microscopic understanding of black hole entropy [5] and other physical properties (see also e.g: the reviews [6, 7]). A related application is in the gauge/gravity correspondence [8, 9], where the near-extremal limits of these black branes give rise to phases in the corresponding dual non-gravitational theories at finite temperature. In this way, finding new black objects can lead to the prediction of new phases in these thermal non-gravitational theories (see e.g: [10, 11]). Finally, if large extra dimensions [12, 13] are realized in Nature, higher-dimensional black holes would be important as possible objects to be produced in accelerators or observed in the Universe (see e.g: the review [14]).

In the past seven years, the two classes that have been studied most intensely are:

- stationary solutions with an event horizon in asymptotically flat space

- static solutions with an event horizon in asymptotically flat spaces with compact directions

For brevity, we will often refer in this lecture to the first type as rotating black holes and the second type as Kaluza-Klein black holes. In this nomenclature, the term "black hole" stands for any object with an event horizon, regardless its horizon topology (i.e: not necessarily spherical). We also allow for the possibility of multiple disconnected event horizons, to which we refer as multi-black hole solutions.

For rotating black holes most progress in recent years has been in five dimensions. Here, it has been found that in addition to the Myers-Perry (MP) black holes [15], there exist rotating black rings [16, 2] and multi-black hole solutions like black-Saturns and multi-black rings [17, 18, 19, 20] including those with two independent angular momenta [21, 22, 23]. All of these are exact solutions which have been obtained with the aid of special ansätze [24, 25] based on symmetries and inverse-scattering techniques [26, 27, 28, 29]. We refer in particular to the review [2] for further details on the black ring in five dimensions and Ref. [18] for a discussion of the phase diagram in five dimensions for the case of rotating black holes with a single angular momentum. Moreover, the very recent review [4] provides a pedagogical overview of black holes in higher dimensions, including the more

general phase structure of five-dimensional stationary black holes and solution generating techniques.

Only recently has there been significant progress in exploring the phase structure of stationary solutions in six and more dimensions [30]. This includes the explicit construction of thin black rings in six and higher dimensions [30] based on a perturbative technique known as matched asymptotic expansion [31, 32, 33, 34, 35]. Furthermore, in Ref. [30] the correspondence between ultra-spinning black holes [36] and black membranes on a two-torus was exploited, to take steps towards qualitatively completing the phase diagram of rotating black folds with a single angular momentum. That has led to the proposal that there is a connection between MP black holes and black rings, and between MP black holes and black Saturns, through merger transitions involving two kinds of 'pinched' black holes. More generally, this analogy suggests an infinite number of pinched black holes of spherical topology leading to a complicated pattern of connections and mergers between phases. The proposed phase diagram was obtained by importing the present knowledge of phase of Kaluza-Klein black holes on a two-torus.

For Kaluza-Klein (KK) black holes, most progress has been for the simplest KK space, namely Minkowski space times a circle. The simplest static solution of Einstein gravity (in five or more dimensions) in this case is the uniform black string, which has a factorized form consisting of a Schwarzschild-Tangherlini black hole and an extra flat (compactified) direction. But there are many more phases of KK black holes, which in recent years have been uncovered by a combination of perturbative techniques (matched asymptotic expansion), numerical methods and exact solutions. These phases include non-uniform black strings (see [37, 38, 39, 40, 41, 42] for numerical results), localized black holes (see [43, 31, 32, 34, 33, 44, 35, 45] for analytical results and [46, 47, 48] for numerical solutions) and bubble-black hole sequences [49]. Here recent progress [35] includes the construction of small mass multi-black hole configurations localized on the circle which in some sense parallel the multi-black hole configurations obtained for rotating black holes.

All of these static, uncharged phases can be depicted in a two-dimensional phase diagram [50, 51, 52] parameterized by the mass and tension. Mapping out this phase structure has consequences for the endpoint of the Gregory-Laamé instability [53, 54] of the neutral black string, which is a long wavelength instability that involves perturbations with an oscillating profile along the direction of the string. The non-uniform black string phase emerges from the uniform black string phase at the Gregory-Laamé point, which is determined by the (time-independent) threshold mode where the instability sets in. An interesting property that has been found in this context is the existence of a critical dimension [39] where the transition of the uniform black string into the non-uniform black string changes from first order into second order. Moreover, it has been shown [55, 56, 57, 41] that the localized black hole phase meets the non-uniform black string phase in a horizon-topology changing merger point. Turning to more recent developments, we note that the new multi-black hole configurations of Ref. [35] raise the question of

existence of new non-uniform black strings. Furthermore, analysis of the three-black hole configuration [35] suggests the possibility of a new class of static lumpy black holes in Kaluza-Klein space.

Many of the insights obtained in this simplest case are expected to carry over as we go to Kaluza-Klein spaces with higher-dimensional compact spaces [58, 59, 3], although the degree of complexity in these cases will increase substantially.

In summary, recent research has shown that in going from four to higher dimensions in vacuum Einstein gravity a very rich phase structure of black holes is observed with fascinating new properties, such as symmetry breaking, new horizon topologies, merger points and in some cases infinite non-uniqueness. Obviously one of the reasons for this richer phase structure is that as the dimension increases there are many more degrees of freedom for the metric. Furthermore, for stationary solutions every time the dimension increases two units, there is one more orthogonal rotation plane available. Another reason is the existence of extended objects in higher dimensions, such as black p-branes (including the uniform black string for $p = 1$). Finally, allowing for compact directions introduces extra scales, and hence more dimensionless parameters in the problem.

The reasons that make the phase structure so rich, such as the increase of the degrees of freedom and the appearance of fewer symmetries, are those that also make it hard to uncover. As the overview above illustrates, there has been remarkable progress in recent years, but we have probably only seen a glimpse of the full phase structure of black holes in higher-dimensional gravity. However, the cases considered so far will undoubtedly provide essential clues towards a more complete picture and will form the basis for further developments into this fascinating subject.

The outline of these lectures is as follows. To set the stage, we first give in Sec. 2 a brief introduction to known uniqueness theorems for black holes in pure gravity and some prominent cases of non-uniqueness in higher dimensions. We also give a short overview of some of the most important techniques that have been used to obtain black hole solutions beyond four dimensions. Then we review the current status for Kaluza-Klein black holes in Secs. 3 and 4. In particular, Sec. 3 presents the main results for black objects on the cylinder with one event horizon as well as results for Kaluza-Klein black holes on a two-torus, which will be relevant in the sequel. Sec. 4 discusses the recently constructed multi-black hole configurations on the cylinder. Then the focus will be turned to rotating black holes in Secs. 5 and 6. The five-dimensional case will be very briefly reviewed, but most attention will be given to the recent progress for six and higher dimensions, including the construction of thin black rings in Sec. 5. We then discuss in Sec. 6 the proposed phase structure for rotating black holes in six and higher dimensions with a single angular momentum. The resulting picture builds on an interesting connection to the phase structure of Kaluza-Klein black holes discussed in the first part. We end with a future outlook for the subject in Sec. 7.

2 Uniqueness theorems and going beyond four dimensions

In this section we first review known black hole uniqueness theorems in Einstein gravity as well as the most prominent cases of non-uniqueness of black holes in higher dimensions. We also give an overview of some of the most important techniques that have been used in finding black hole solutions beyond four dimensions.

2.1 Black hole (non-)uniqueness

The purpose of this lecture is to explore possible black hole solutions of the vacuum Einstein equations $R = 0$ in dimensions $D \geq 4$. In four-dimensional vacuum gravity, a black hole in an asymptotically flat space-time is uniquely specified by the ADM mass M and angular momentum J measured at infinity [60, 61, 62, 63]. In particular, in the static case the unique solution is the four-dimensional Schwarzschild black hole solution, and for the stationary case it is the Kerr black hole

$$ds^2 = -dt^2 + \frac{r}{\Delta} (dt + a \sin^2 \theta d\phi)^2 + \Delta^{-1} dr^2 + \Delta d\theta^2 + (r^2 + a^2) \sin^2 \theta d\phi^2; \quad (1a)$$

$$\Delta = r^2 + a^2 \cos^2 \theta; \quad r_{\pm} = r^2 \pm 2Mr \pm a^2; \quad \Delta = 2GM; \quad a = \frac{J}{M}; \quad (1b)$$

For $J = 0$ this clearly reduces to the Schwarzschild black hole, and the angular momentum is bounded by a critical value $J \leq GM^2$ (the Kerr bound) beyond which there appears a naked singularity. The bound is saturated for the extremal Kerr solution which is non-singular. The uniqueness in four dimensions fits nicely with the fact that black holes in four dimensions are known to be classically stable [64, 65, 66] (for further references see also the lecture [67] at this school).

The generalization of the Schwarzschild black hole to arbitrary dimension D was found by Tangherlini [68], and is given by the metric

$$ds^2 = -f dt^2 + f^{-1} dr^2 + r^2 d\Omega_{D-2}^2; \quad f = 1 - \frac{r_0^D}{r^{D-3}}; \quad (2)$$

Here $d\Omega_{D-2}^2$ is the metric element of a $(D-2)$ -dimensional unit sphere with volume $\Omega_{D-2} = 2\pi^{D/2} \Gamma(D/2) = [(D-1)!/2]$. Since the Newtonian potential in the weak-field regime $r \gg r_0$ can be obtained from $g_{tt} = -1 - 2\Phi$, this shows that $\Phi = -\frac{r_0^D}{2r^{D-3}}$. The mass of the black hole is then easily obtained as

$$M = \frac{D-2}{16\pi G} \frac{(D-2)}{r_0^{D-3}}; \quad (3)$$

by using $r^2 \Phi = 8\pi G \frac{D-3}{2} T_{tt}$ and $M = \int dx^{D-1} T_{tt}$ where T_{tt} is the energy density. Uniqueness theorems [69, 70] for D -dimensional ($D > 4$) asymptotically flat space-times state that the Schwarzschild-Tangherlini black hole solution is the only static black hole in pure gravity. The classical stability of these higher-dimensional black hole solutions was addressed in Refs. [71, 72, 73].

The generalization of the Kerr black hole (1) to arbitrary dimension D was found by Myers and Perry [15], who obtained the metric of a rotating black hole with angular momenta in an arbitrary number of orthogonal planes. The Myers-Perry (MP) black hole is thus specified by the mass and angular momenta J_k where $k = 1 :: r$ with $r = \text{rank}(SO(D-2))$. For MP black holes with a single angular momentum, there is again a Kerr bound $J^2 < 32GM^3$ (27) in the D -dimensional case, but for six and more dimensions the angular momentum is unbounded, and the black hole can be ultra-spinning. This fact will be important in Secs. 5 and 6. When there are more than one angular momenta one needs at least one or two zero angular momenta to have an ultra-spinning regime depending on whether the dimension is even or odd [36].

Despite the absence of a Kerr bound in six and higher dimensions, it was argued in [36] that in six or higher dimensions the Myers-Perry black hole becomes unstable above some critical angular momentum thus recovering a dynamical Kerr bound. The instability was identified as a Gregory-Laflamme instability by showing that in a large angular momentum limit the black hole geometry becomes that of an unstable black membrane. This result is also an indication of the existence of new rotating black holes with spherical topology, where the horizon is distorted by ripples along the polar direction. This will be discussed in more detail in Sec. 6. Finally, we note that all of the black hole solutions discussed so far in this section have an event horizon of spherical topology S^{D-2} .

Contrary to the static case, there are no uniqueness theorems for non-static black holes in pure gravity with $D > 4$.¹ On the contrary, there are known cases of non-uniqueness. The first example of this was found by Emparan and Reall [16] and occurs in D dimensions for stationary solutions in asymptotically flat space-time: for a certain range of mass and angular momentum there exist both a rotating MP black hole with S^3 horizon [15] and rotating black rings with $S^2 \times S^1$ horizons [16].

As mentioned in the introduction, following the discovery of the rotating black ring [16], further generalizations of these to black Saturns and multi-black rings have been found in D dimensions. It is possible that essentially all D -dimensional black holes (up to iterations of multi-black rings) with two axial Killing vectors have been found by now², but the study of non-uniqueness for rotating black holes in six and higher dimensions has only recently begun (see Secs. 5 and 6).

Another case where non-uniqueness has been observed is for Kaluza-Klein black holes, in particular for black hole solutions that asymptote to Minkowski space M^{D-1} times a circle S^1 . Here, the simplest solution one can construct is the uniform black string which is the $(D-1)$ -dimensional Schwarzschild-Tangherlini black hole (2) plus a flat direction, which has horizon topology $S^{D-3} \times S^1$. However, at least for a certain range of masses, there are also non-uniform black strings and black holes that are localized on the circle, both of which are non-translationally invariant along the circle direction.

¹See [74] for recent progress in this direction.

²See [75, 76] for work on how to determine uniquely the black hole solutions with two symmetry axes.

All of these solutions, which have in common that they possess an $SO(D-2)$ symmetry, will be further discussed in Sec. 3. If one allows for disconnected horizons, then also multi-black hole configurations localized on the circle are possible, giving rise to a finite non-uniqueness. These will be discussed in Sec. 4. In addition there are more exotic black hole solutions, called bubble-black hole sequences [49], but for simplicity these will not be further dealt with in this lecture.

More generally, for black hole solutions that asymptote to Minkowski space M^{D-p} times a torus T^p , the simplest class of solutions with an event horizon are black p-branes. The metric is that of a $(D-p)$ -dimensional Schwarzschild-Tangherlini black hole \mathcal{B} plus p flat directions. Beyond that there will exist many more phases, which have only been partially explored. As an example, we discuss in Sec. 3.4 the phases of KK black holes on T^2 that follow by adding a flat direction to the phases of KK black holes on S^1 . These turn out to be intimately related to the phase structure of rotating black holes for $D=6$, as we will see in Sec. 6.

2.2 Overview of solution methods

We briefly describe here the available methods that have been employed in order to find the new solutions that are the topic of this lecture. The main techniques for finding new solutions are as follows.

Symmetries and ansätze. It is often advantageous to use symmetries and other physical input to constrain the form of the metric for the putative solution. In this way one may be able to find an ansatz for the metric that enables to solve the vacuum Einstein equations exactly. This often involves also a clever choice of coordinate system, adapted to the symmetries of the problem. This ingredient is also important in cases where the Einstein equations can only be solved perturbatively around a known solution (see below).

As an example we note the generalized Weyl ansatz [24, 25] for static and stationary solutions with $D-2$ commuting Killing vectors, in which the Einstein equations simplify considerably. For the static case, this ansatz is for example relevant for bubble-black hole sequences [49] in five and six-dimensional KK space. For the stationary case, it is relevant for rotating black ring solutions in five dimensional asymptotically flat space. Another example relevant for black holes and strings on cylinders is the $SO(D-2)$ -symmetric ansatz of [43, 56, 52] based on coordinates that interpolate between spherical and cylindrical coordinates [43]. This has been used to obtain the metric of small black holes on the cylinder [31, 35].

Solution generating techniques. Given an exact solution there are cases where one can use solution generating techniques, such as the inverse scattering method, to generate other new solutions. See for example Refs. [26, 27, 28, 29] where this method was first used for stationary black hole solutions in five dimensions, and [77] for a further solution generating mechanism.

Matched asymptotic expansion. In some cases one knows the exact form of the solution in some corner of the moduli space. Then one may attempt to find the solution in a perturbative expansion around this (limiting) known solution. This method, called matched asymptotic expansion [31, 32, 33, 34, 35, 30], has been very successful. It applies to problems that contain two (or more) widely separated scales. In particular for black holes, this means that one solves Einstein equations perturbatively in two different zones, the asymptotic zone and the near-horizon zone and one thereafter matches the solution in the overlap region. One example is that of small black holes on a circle, where the horizon radius of the black holes is much smaller than the size of the circle (see in particular Sec. 4). Another example is that of thin black rings, where the thickness of the ring is much smaller than the radius of the ring (see Sec. 5).

Numerical techniques. Since in many cases the Einstein equations become too complicated to be amenable to analytical methods, even after using symmetries and ansätze, the only way to proceed in the non-linear regime is to try to solve them numerically. Especially for KK black holes these techniques have been successfully applied for non-uniform black strings [37, 38, 39, 40, 41, 42] and localized black holes [46, 47, 48] (see Sec. 3).

Classical effective field theory. There exists also a classical effective field theory approach for extended objects in gravity [78]. This can be used as a systematic low-energy (long-distance) effective expansion which gives results only in the region away from the black hole and so it does not provide the corrections to the metric near the horizon, but enables one to compute perturbatively corrected asymptotic quantities. This has been successfully applied in [44] to obtain the second-order correction to the thermodynamics of small black holes on a circle. Recently, it was shown [45] that this method is equivalent to matched asymptotic expansion where the near-horizon zone is replaced by an effective theory. Ref. [45] also contains an interesting new application of the method to the corrected thermodynamics of small MP black holes on a circle.

3 Kaluza-Klein black holes

In this section we give a general description of the phases of Kaluza-Klein (KK) black holes (see also the reviews [3, 79]). A $(d+1)$ -dimensional Kaluza-Klein black hole will be defined here as a pure gravity solution with at least one event horizon that asymptotes to d -dimensional Minkowski space times a circle ($M^d \times S^1$) at infinity. We will discuss only static and neutral solutions, i.e.: solutions without charges and angular momenta. Obviously, the uniform black string is an example of a Kaluza-Klein black hole, but many more phases are known to exist. In particular, we discuss here the non-uniform black string and the localized black hole phase. Finally, in anticipation of the connection with the phase structure of rotating black holes (discussed in Sec. 6) we also discuss part of the phases of KK black holes on Minkowski space times a torus ($M^{D-2} \times T^2$).

3.1 Setup and physical quantities

For any space-time which asymptotes to $M^{d-1} \times S^1$ we can define the mass M and the tension T . These two asymptotic quantities can be used to parameterize the various phases of Kaluza-Klein black holes in a $(d; n)$ phase diagram, as we review below.

The Kaluza-Klein space $M^{d-1} \times S^1$ consists of the time t and a spatial part which is the cylinder $R^{d-1} \times S^1$. The coordinates of R^{d-1} are x^1, \dots, x^{d-1} and the radius $r = \sqrt{\sum_i (x^i)^2}$. The coordinate of the S^1 is denoted by z and its circumference is L . It is well known that for static and neutral mass distributions in flat space R^d the leading correction to the metric at infinity is given by the mass. For a cylinder $R^{d-1} \times S^1$ we instead need two independent asymptotic quantities to characterize the leading correction to the metric at infinity.

Mass and tension. Consider a static and neutral distribution of matter which is localized on a cylinder $R^{d-1} \times S^1$. Assume a diagonal energy momentum tensor with components T_{tt} , T_{zz} and T_{ii} . Here T_{tt} depends on $(x^i; z)$ while T_{zz} depends only on x^i because of momentum conservation. We can then write the mass and tension as

$$M = \int_{S^1} dx^{d-1} T_{tt}; \quad T = \frac{1}{L} \int_{S^1} dx^{d-1} T_{zz} : \quad (4)$$

From these definitions and the method of equivalent sources, one can obtain expressions for M and T in terms of the leading $1=r^{d-3}$ behavior of the metric components g_{tt} and g_{zz} around flat space [50, 51]. See also Refs. [80, 11, 81, 82, 83, 84] for more on the gravitational tension of black holes and branes.

For a neutral Kaluza-Klein black hole with a single connected horizon, we can find the temperature T and entropy S directly from the metric. Together with the mass M and tension T , these quantities obey the Smarr formula [50, 51]

$$(d-1)TS = (d-2)M - LT; \quad (5)$$

and the first law of thermodynamics [83, 51, 52]

$$M = T S + T L; \quad (6)$$

This equation includes a "work" term (analogous to pV) for variations with respect to the size of the circle at infinity.

It is important to note that there are also examples of Kaluza-Klein black hole solutions with more than one connected event horizon [52, 49, 35]. The Smarr formula (5) and first law of thermodynamics (6) generalize also to these cases.

Dimensionless quantities. Since for KK black holes we have an intrinsic scale L it is natural to use it in order to define dimensionless quantities, which we take as

$$m = \frac{16 G}{L^{d-2}} M; \quad s = \frac{16 G}{L^{d-1}} S; \quad t = LT; \quad n = \frac{TL}{M}; \quad (7)$$

Here ρ , s and t are the rescaled mass, entropy and temperature respectively, and n is the relative tension. The relative tension satisfies the bound $0 < n < d/250$. The upper bound is due to the Strong Energy Condition whereas the lower bound was found in [85, 86]. The upper bound can also be understood physically in a more direct way from the fact that we expect gravity to be an attractive force. For a test particle at infinity it is easy to see that the gravitational force on the particle is attractive when $n < d/2$ but repulsive when $n > d/2$.

The program set forth in [50, 52] is to plot all phases of Kaluza-Klein black holes in a $(\rho; n)$ diagram. Note that it follows from the Smarr formula (5) and the first law of thermodynamics (6) that given a curve $n(\rho)$ in the phase diagram, the entire thermodynamics $s(\rho)$ of a phase can be obtained [50]. We also note that the $(\rho; n)$ phase diagram appears to be divided into two separate regions [49]. Here, the region $0 < n = 1/(d-2)$ contains solutions without Kaluza-Klein bubbles, and the solutions have a local $SO(d-1)$ symmetry and reside in the ansatz proposed in [43, 87] and proven in [56, 52]. Solutions of this type, also referred to as black holes and strings on cylinders will be reviewed in Sec. 3.2. Because of the $SO(d-1)$ symmetry there are only two types of event horizon topologies: S^{d-1} for the black hole on a cylinder branch and $S^{d-2} \times S^1$ for the black string. The region $1/(d-2) < n < d/2$ contains solutions with Kaluza-Klein bubbles. This part of the phase diagram, which is much more densely populated with solutions compared to the lower part, is the subject of [49].

Alternative dimensionless quantities. The typical dimensionless quantities used for KK black holes in D dimensions, are those defined in (7). Instead of these, Ref. [30] introduced the following new dimensionless quantities, more suitable for the analogy with rotating black holes (see Sec. 6), by defining

$$\rho^{D-3} / \frac{L^{D-3}}{GM}; \quad a_H^{D-3} / \frac{S^{D-3}}{(GM)^{D-2}}; \quad t_H / (GM)^{\frac{1}{D-3}} T : \quad (8)$$

In particular, the relation to the dimensionless quantities in (7) is given by

$$\rho = \frac{1}{d-3}; \quad a_H = \frac{d-2}{d-3} s; \quad t_H = \frac{1}{d-3} t : \quad (9)$$

In the KK black hole literature, entropy plots are typically given as $s(\rho)$. Instead of these one can also use (9) to consider the area function $a_H(\rho)$, which is obtained as

$$a_H(\rho) = \rho^{D-2} s(\rho^{D+3}) : \quad (10)$$

We will employ these alternative quantities when we discuss KK black holes on a torus in Sec. 3.4

3.2 Black holes and strings on cylinders

We now discuss the main three types of KK black holes that have $SO(d-1)$ symmetry, to which we commonly refer as black holes and strings on cylinders. These are the uniform

black string, the non-uniform black string and the localized black hole. In Sec. 4 we will discuss in more detail the recently obtained multi-black hole configurations on the cylinder.

Uniform black string and Gregory-Laamme instability

The metric for the uniform black string in $D = d + 1$ space-time dimensions is

$$ds^2 = -f dt^2 + f^{-1} dr^2 + r^2 d\Omega_{d-2}^2 + dz^2; \quad f = 1 - \frac{r_0^{d-3}}{r^{d-3}}; \quad (11)$$

where $d\Omega_{d-2}^2$ is the metric element of a $(d-2)$ -dimensional unit sphere. The metric (11) is found by taking the d -dimensional Schwarzschild-Tangherlini static black hole (2) solution [68] and adding a z direction, which is the direction parallel to the string. The event horizon is located at $r = r_0$ and has topology $S^{d-2} \times \mathbb{R}$.

Gregory-Laamme instability. Gregory and Laamme found in 1993 a long wavelength instability for black strings in five or more dimensions [53, 54]. The mode responsible for the instability propagates along the direction of the string, and develops an exponentially growing time-dependent part when its wavelength becomes sufficiently long. The Gregory-Laamme mode is a linear perturbation of the metric (11), that can be written as

$$g + h; \quad (12)$$

Here g stands for the components of the unperturbed black string metric (11), ϵ is a small parameter and h is the metric perturbation

$$h = \langle \exp \left[\frac{t}{r_0} + i \frac{kz}{r_0} \right] P(r=r_0) \rangle; \quad (13)$$

where the symbol \langle denotes the real part. The statement that the perturbation h of g satisfies the Einstein equations of motion can be stated as the differential operator equation

$$\Delta_L h = 0; \quad (14)$$

where $(\Delta_L) = \square_g + 2R$ is the Lichnerowicz operator for the background metric g . The resulting Einstein equations for the GL mode can be found e.g. in the appendix of the review [3].³ Solution of these equations [53, 54] shows that there is an unstable mode for any wavelength larger than the critical wavelength

$$\lambda_{GL} = \frac{2 r_0}{k_c}; \quad (15)$$

for which $\epsilon = 0$ in (13). The values of k_c for $d = 4, \dots, 14$, as obtained in [53, 37, 39], are listed e.g. in Table 1 of [3]. The critical wave-number k_c marks the lower bound of the possible wavelengths for which there is an unstable mode and is called the threshold

³Various methods and different gauges have been employed to derive the differential equations for the GL mode. See Ref. [68] for a nice summary of these, including a new derivation (see also [69]).

mode. It is a time-independent mode of the form $h_c \exp(ik_z z = r_0)$. In particular, this suggests the existence of a static non-uniform black string.

GL mode of the compactified uniform black string. Since we wish to consider the uniform black string in KK space, we now discuss what happens to the GL instability when z is a periodic coordinate with period L . The Gregory-Laamé mode (13) cannot obey the correct periodic boundary condition on z if $L < \ell_{GL}$, with ℓ_{GL} given by (15). On the other hand, for $L > \ell_{GL}$, we can fit the Gregory-Laamé mode into the compact direction with the frequency and wave number and k in (13) determined by the ratio $r_0 = L$. Translating this in terms of the mass of the neutral black string, one finds the critical Gregory-Laamé mass

$$\ell_{GL} = (d-2) \frac{d-2}{2} \frac{k_c}{\omega_c} : \quad (16)$$

For $L < \ell_{GL}$ the Gregory-Laamé mode can be fitted into the circle, and the compactified neutral uniform black string is unstable. For $L > \ell_{GL}$, on the other hand, the Gregory-Laamé mode is absent, and the neutral uniform black string is stable. For $L = \ell_{GL}$ there is a marginal mode which signals the emergence of a new branch of black string solutions which are non-uniformly distributed along the circle. See e.g. Table 2 in [3] for the values of ℓ_{GL} for $4 \leq d \leq 14$.

The large d behavior of ℓ_{GL} was examined numerically in [39] and analytically in [58]. We also note that there is an interesting correspondence between the Rayleigh-Plateau instability of long fluid cylinders and the Gregory-Laamé instability of black strings [90, 91]. In particular, the critical wave numbers k_{RP} and k_c agree exactly at large dimension d (scaling both as $\frac{1}{d}$ for $d \gg 1$).

Non-uniform black string

It was realized in [37] (see also [92]) that the classical instability of the uniform black string for $L < \ell_{GL}$ implies the existence of a marginal (threshold) mode at $L = \ell_{GL}$, which again suggests the existence of a new branch of solutions.

The new branch, which is called the non-uniform string branch, has been found numerically in [37, 38, 39]. This branch of solutions has the same horizon topology $S^1 \times S^{d-2}$ as the uniform string, which is expected since the non-uniform string is continuously connected to the uniform black string. In particular, it emerges from the uniform black string in the point $(\ell; n) = (\ell_{GL}; 1 = (d-2))$ and has $n < 1 = (d-2)$. Moreover, the solution is non-uniformly distributed in the circle-direction z since there is an explicit dependence in the marginal mode on this direction.

More concretely, considering the non-uniform black string branch for $j = \ell_{GL} j - 1$ one obtains for the relative tension the behavior

$$n(\ell) = \frac{1}{d-2} (\ell - \ell_{GL}) + O((\ell - \ell_{GL})^2) : \quad (17)$$

Here β is a number representing the slope of the curve that describes the non-uniform string branch near $\mu = \mu_{GL}$ (see Table 3 in [3] for the values of β for $4 \leq d \leq 14$ obtained from the data of [53, 54, 37, 38, 39]).

The qualitative behavior of the non-uniform string branch depends on the sign of β . If β is positive, then the branch emerges at the mass $\mu = \mu_{GL}$ with increasing μ and decreasing n . If instead β is negative the branch emerges at $\mu = \mu_{GL}$ with decreasing μ and decreasing n . To see what this means for the entropy we note that from (17) and the first law of thermodynamics one finds

$$\frac{s_{nu}(\mu)}{s_u(\mu)} = 1 - \frac{(d-2)^2}{2(d-1)(d-3)} \frac{1}{\mu_{GL}} (\mu - \mu_{GL})^2 + O((\mu - \mu_{GL})^3); \quad (18)$$

where $s_u(\mu)$ ($s_{nu}(\mu)$) refers to the rescaled entropy of the uniform (non-uniform) black string branch. It turns out that β is positive for $d \leq 12$ and negative for $d \geq 13$ [39]. Therefore, as discovered in [39], the non-uniform black string branch has a qualitatively different behavior for small d and large d , i.e.: the system exhibits a critical dimension $D = 14$. In particular, for $d \leq 12$ the non-uniform branch near the GL point has $\mu > \mu_{GL}$ and lower entropy than that of the uniform phase, while for $d > 13$ it has $\mu < \mu_{GL}$ and higher entropy. It also follows from (18) that for all d the curve $s_{nu}(\mu)$ is tangent to the curve $s_u(\mu)$ at the GL point.

A large set of numerical data for the non-uniform branch, extending into the strongly non-linear regime, have been obtained in Refs. [38, 48] for six dimensions (i.e.: $d = 5$) in Ref. [40] for five dimensions (i.e.: $d = 4$) and for the entire range $d = 5 - 10$ in Ref. [41]. For $d = 5$, these data are displayed in the $(\mu; n)$ phase diagram [50] of Fig. 1.

Localized black holes

On physical grounds, it is natural to expect a branch of neutral black holes in the space-time $M^{d-1} \times S^1$ with event horizon of topology S^{d-1} . This branch is called the localized black hole branch, because the S^{d-1} horizon is localized on the S^1 of the Kaluza-Klein space.

Neutral black hole solutions in the space-time $M^{d-3} \times S^1$ were found and studied in [93, 94, 95, 96]. However, the study of black holes in the space-time $M^{d-1} \times S^1$ for $d \geq 4$ is relatively new. The complexity of the problem stems from the fact that such black holes are not algebraically special [97] and moreover from the fact that the solution cannot be found using a Weyl ansatz since the number of Killing vectors is too small.

In [31, 32, 34] the metric of small black holes, i.e.: black holes with mass $\mu \ll 1$, was found analytically using the method of matched asymptotic expansion. The starting point in this construction is the fact that as $\mu \rightarrow 0$, one has $n \rightarrow 0$ so that the localized black hole solution becomes more and more like a $(d+1)$ -dimensional Schwarzschild black hole in this limit. For $d = 4$, the second order correction to the metric and thermodynamics have been studied in [33]. More generally, the second order correction to the thermodynamics

was obtained in Ref. [44] (see also [45]) for all d using an effective field theory formalism in which the structure of the black hole is encoded in the coefficients of operators in an effective worldline Lagrangian.

The first order result of [31] and second order result of [44] can be summarized by giving the first and second order corrections to the relative tension n of the localized black hole branch as a function of

$$n = \frac{(d-2)(d-2)}{2(d-1)d} + \frac{(d-2)(d-2)}{2(d-1)d} \epsilon^2 + O(\epsilon^3); \quad (19)$$

where $\zeta(p) = \sum_{n=1}^{\infty} n^{-p}$ is the Riemann zeta function. The corresponding correction to the thermodynamics can be found e.g. in Eq. (3.18) of [3].

The black hole branch has been studied numerically for $d=4$ in [46, 48] and for $d=5$ in [47, 48]. For small ϵ , the impressively accurate data of [48] are consistent with the analytical results of [31, 32, 33]. The results of [48] for $d=5$ are displayed in a $(\epsilon; n)$ phase diagram in Figure 1.

3.3 Phase diagram and copied phases

In Figure 1 the $(\epsilon; n)$ diagram for $d=5$ is displayed, which is one of the cases most information is known. We have shown the complete non-uniform branch, as obtained numerically by Wiseman [38], which emanates at $\epsilon_L = 2.31$ from the uniform branch that has $n=1/3$. These data were first incorporated into the $(\epsilon; n)$ diagram in Ref. [50]. For the black hole branch we have plotted the numerical data of Kudoh and Wiseman [48]. It is evident from the figure that this branch has an approximate linear behavior for a fairly large range of ϵ close to the origin and the numerically obtained slope agrees very well with the analytic result (19).

Merger point. The figure strongly suggests that the localized black hole branch meets with the non-uniform black string branch in a topology changing transition point, which is the scenario earlier suggested by Kol [55] (see [52] for a list of scenarios). For this reason, it seems reasonable to expect that the localized black hole branch is connected with the non-uniform string branch in any dimension. This means that we can go from the uniform black string branch to the localized black hole branch through a connected series of static classical geometries. The point in which the two branches are conjectured to meet is called the merger point.

Copied phases. In [52] it was shown that one can generate new solutions by copying solutions on the circle several times, following an idea of Horowitz [98]. This works for solutions which vary along the circle direction (i.e. in the z direction), so it works both for the black hole branch and the non-uniform string branch. Let k be a positive integer. Then if we copy a solution k times along the circle we get a new solution with the following parameters:

$$\tilde{\epsilon} = \frac{\epsilon}{k^{d-3}}; \quad \tilde{s} = \frac{s}{k^{d-2}}; \quad \tilde{t} = kt; \quad \tilde{n} = n; \quad (20)$$

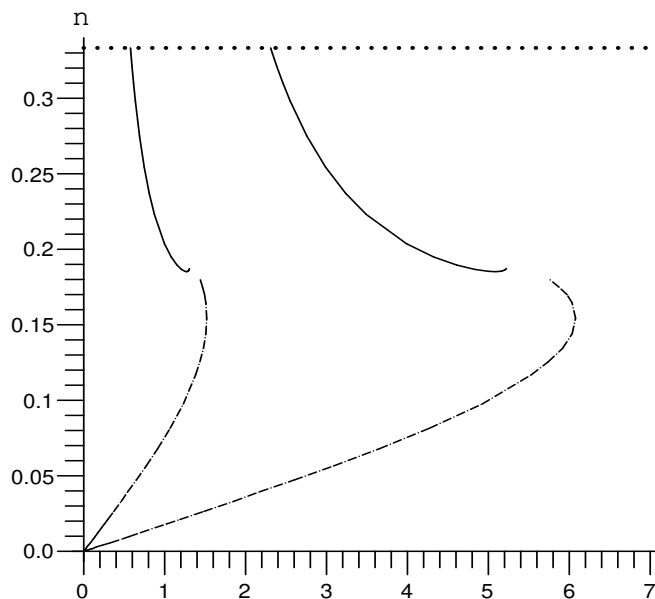


Figure 1: Black hole and string phases for $d = 5$, drawn in the $(g; n)$ phase diagram. The horizontal (dotted) line is the uniform string branch. The rightmost solid branch emanating from this at the Gregory-Laamance point is the non-uniform string branch and the rightmost dashed branch starting in the origin is the localized black hole branch. The solid and dashed branches to the left are the $k = 2$ copies of the non-uniform and localized branch. The results strongly suggest that the black hole and non-uniform black string branches meet.

See Ref. [52] for the corresponding expression of the metric of the copies in the $SO(d-1)$ -symmetric ansatz. Using the transformation (20), one easily sees that the non-uniform and localized black hole branches depicted in Fig. 1 are copied infinitely many times in the $(g; n)$ phase diagrams, and we have depicted the $k = 2$ copy in this figure.

General dimension. The six-dimensional phase diagram displayed in Fig. 1 is believed to be representative for the black string/localized black hole phases on $M^{D-1} \times S^1$ for all $5 \leq D \leq 13$. Here the upper bound follows from the fact that, as mentioned above, there is a critical dimension $D = 13$ above which the behavior of the non-uniform black string phase is qualitatively different [39]. The phase diagram for $D = 14$ is much poorly known in comparison, since there are no data like Fig. 1 available for the localized and non-uniform phases, only the asymptotic behaviors. However, we do know from (17) that the non-uniform branch will extend to the left (lower values of g) as it emerges from the GL point, and on general grounds is expected to merge again with the localized black hole branch.

3.4 KK phases on T^2 from phases on S^1

We show here how one can translate the known results for KK black holes on the circle (i.e. on $M^{D-2} \times S^1$) to results for KK black holes on the torus (i.e. on $M^{D-2} \times T^2$). The resulting phases are relevant in connection with the phases of rotating black holes in asymptotically flat spacetime, as shown in Sec 6.

We recall first the definitions of dimensionless quantities in (7). While these quantities were originally introduced in [50, 11] for black holes on a KK circle of circumference L , we may similarly use these definitions for KK black holes in D dimensions with a square torus of side lengths L , to which we restrict in the following. Likewise, we can use the alternative dimensionless quantities (9) for that case.

Map from circle to torus compactification. We first want to establish a map for these dimensionless quantities from KK black holes on $M^{D-2} \times S^1$ (denoted with hatted quantities) to those for KK black holes on $M^{D-2} \times T^2$ (denoted with unhatted quantities), obtained by adding an extra compact direction of size L . Suppose we are given an entropy function $\hat{s}(\hat{\nu})$ for a phase of KK black holes on $M^{D-2} \times S^1$. Any such phase lifts trivially to a phase of KK black holes on $M^{D-2} \times T^2$ that is uniform in one of the torus directions. We show below how to obtain the function $a_H(\nu)$ for the latter in terms of $\hat{s}(\hat{\nu})$ of the former. In the following we will use the notation $D = n + 4$.

It is not difficult to see that in terms of the original dimensionless quantities (7) we have the simple mapping

$$\nu = \hat{\nu}; \quad s = \hat{s}; \quad t = \hat{t}; \quad (21)$$

It then follows from (9) and (10) that the area function $a_H(\nu)$ of KK black holes on $M^{D-2} \times T^2$ is obtained via the mapping relation

$$a_H(\nu) = \nu^{n+2} \hat{s}(\hat{\nu}^{n-1}); \quad (22)$$

Application to known phases. Using now the entropy function $\hat{s}_{\text{uni}}(\hat{\nu}) \sim \hat{\nu}^{\frac{n}{n-1}}$ of the uniform black string in $M^{n+2} \times S^1$ we get from (22) the result

$$a_H^{\text{ubm}}(\nu) \sim \nu^{\frac{2}{n-1}}; \quad (23)$$

for the uniform black membrane (ubm) $4+n$ dimensions. Furthermore, using that for small ν (or equivalently large $\hat{\nu}$) the entropy of the localized black hole in $M^{n+2} \times S^1$ is $\hat{s}_{\text{loc}}(\hat{\nu}) \sim \hat{\nu}^{\frac{n+1}{n}}$ we find via the map (22) the result

$$a_H^{\text{lbs}}(\nu) \sim \nu^{\frac{1}{n}} (\nu \gg 1); \quad (24)$$

for the large ν limit of the localized black string (lbs) in $4+n$ dimensions.

Finally, for the non-uniform string in $M^{n+2} \times S^1$ dimensions we use (18) to obtain

$$a_H^{\text{nubm}}(\nu) = a_H^{\text{ubm}}(\nu) \left[1 - \frac{n^2(n+1)}{2(n-1)^2} \frac{n+2}{\nu_{GL}^{n+4}} (\nu_{GL})^2 + O((\nu_{GL})^3) \right]; \quad (25)$$

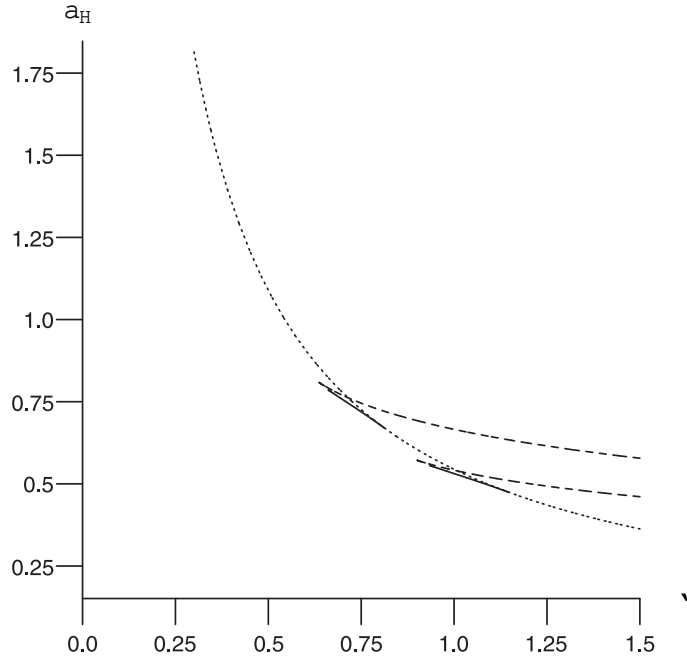


Figure 2: a_H (λ) phase diagram in seven dimensions ($M^5 \times T^2$) for Kaluza-Klein black hole phases with one uniform direction. Shown are the uniform black membrane phase (dotted), the non-uniform black membrane phase (solid) and the localized black string phase (dashed). For the latter two phases, we have also shown their $k = 2$ copy. The non-uniform black membrane phase emanates from the uniform black membrane phase at the GL point $\lambda_{GL} = 0.811$, while the $k = 2$ copy starts at the 2-copied GL point $\lambda_{GL}^{(2)} = \sqrt{2} \lambda_{GL} = 1.15$. This figure is representative for the phase diagram of phases on $M^{D-2} \times T^2$ for all $6 \leq D \leq 14$. Reprinted from Ref. [30].

for the non-uniform black membrane (nubm). Here, $\lambda_{GL} = (\lambda_{GL, n+2})^{\frac{1}{n+1}}$ is the critical GL wavelength in terms of the dimensionless GL mass $\lambda_{GL, n+2}$ given in (16) and α_d the coefficient in (17).

Copies. As remarked in Sec. 3.3 the localized black hole and non-uniform black string phase on $M^{n+2} \times S^1$ have copied phases with multiple non-uniformity or multiple localized black objects. From the map (20) we then find using (21) and the definitions (9) that corresponding copied phases of KK black holes on the torus obey the transformation rule

$$\lambda = k^{\frac{n-1}{n+1}} \lambda'; \quad a_H = k^{\frac{2}{n+1}} a_H'; \quad \lambda_H = k \lambda_H' : \quad (26)$$

Seven-dimensional phase diagram. As an explicit example, we give the mapping that can be used to convert the known results for KK black holes on $M^5 \times S^1$ to KK black holes on $M^5 \times T^2$.

$$(\lambda'; a_H') = (\lambda^{\wedge 1=4}; a_H^{\wedge 5=4}) : \quad (27)$$

This can be used to convert plots of points $(\lambda; a_H)$ (see e.g. [3]) for six-dimensional KK black holes on a circle to the phase diagram in Fig. 2 for seven-dimensional KK black

holes (with one uniform direction) on a torus. It includes the uniform black membrane, the black membrane with one uniform and one non-uniform direction, and the black string localized in one of the circles of T^2 . The figure also includes the $k = 2$ copies obtained from these data and the map (26). Both the uniform black membrane phase and the localized black string phase extend to $\ell = 1$ where they obey the behavior (23) and (24) respectively with $n = 3$.

4 Multi-black hole configurations on the cylinder

We now turn to the construction of multi-black hole configurations on the cylinder, recently obtained in Ref. [35]. In Sec. 3.3 we already encountered a special subset of these, namely the copied phases of the localized black hole branch, corresponding to multi-black hole configurations in which all black holes have the same mass. Here, we describe the main points of the construction of more general multi-black hole configurations [35] using matched asymptotic expansion. We also show how the thermodynamics of these configurations can be understood from a Newtonian point of view. Finally we comment on the consequences of these configurations for the phase diagram of KK black holes.

4.1 Construction of multi-black hole solutions

The copies of the single-black hole localized on the circle, correspond to a multi-black hole configurations of equal mass black holes that are spread with equal distance from each other on the circle. Beyond these, there exist more general multi-black hole configurations which have recently been considered in Ref. [35]. These solutions correspond to having several localized black holes of different sizes located at different points along the circle direction of the cylinder $R^{d-1} \times S^1$. The location of each black hole is such that the total force on each of them is zero, ensuring that they are in equilibrium. It is moreover necessary for being in equilibrium that the black holes are all located in the same point in the R^{d-1} part of the cylinder.

The metric constructed in Ref. [35] are solutions to the Einstein equations to first order in the mass. More precisely, they are valid in a regime where the gravitational interaction between any one of the black holes and the others (and their images on the circle) is small. The solutions in Ref. [35] thus describe the small mass limit of these multi-black hole configurations on the cylinder, or equivalently they can be said to describe the situation where the black holes are far apart. The method used for solving the Einstein equations is the one of matched asymptotic expansion [31, 32, 33, 34, 35]. The particular construction follows the approach of [31] where it was used to find the metric of a small black hole on the cylinder based on an ansatz for the metric found in [43].

General idea and starting point. We describe here the general idea behind constructing the new solutions for multi-black hole configurations on the d -dimensional cylinder

$R^{d-1} \times S^1$. The configuration under consideration is that of k black holes placed at different locations $z_i, i = 1 :: k$ in the same point of the R^{d-1} part of the cylinder. We write M as the total mass of all of the black holes and define α_i as the fraction of mass of the i^{th} black hole, i.e:

$$M \alpha_i = \sum_{i=1}^k M_i ; \quad \sum_{i=1}^k \alpha_i = 1 ; \quad (28)$$

where M_i is the mass of the i^{th} black hole. Note that $0 < \alpha_i \leq 1$.

The matched asymptotic expansion is suitable when there are two widely separated scales in the problem. Here they are the size (mass) of each of the black holes, (all of which are taken of the same order) and the length of the circle direction. In particular, we assume that all black holes have a horizon radius (of the same order) which is small compared to the length of the circle.

The constructing of the solution then proceeds in the following steps⁴

Step 1: Find a metric corresponding to the Newtonian gravitational potential sourced by a configuration of small black holes on the cylinder. This metric is valid in the region $R_0 \ll R \ll L$.

Step 2: Consider the Newtonian solution close to the sources, i.e: in the overlap region $R_0 \ll R \ll L$.

Step 3: Find a general solution near a given event horizon and match this solution to the metric in the overlap region found in Step 2. The resulting solution is valid in the region $R_0 \ll R \ll L$.

With all these three steps implemented, we have a complete solution for all of the spacetime outside the event horizon. We refer to Ref. [35] for further details, including the explicit form of the first-order corrected metric and thermodynamics of the resulting multi-black hole configurations, but present some of the easy steps here.

Newtonian potential. Following the discussion in Sec. 3.1 for static solutions on the cylinder the two relevant components of the stress tensor are T_{tt} and T_{zz} . These components source the two gravitational potentials [50]

$$\nabla^2 \Phi = 8 \pi G \frac{d-2}{d-1} T_{tt} ; \quad \nabla^2 B = \frac{8 \pi G}{d-1} T_{zz} ; \quad (29)$$

where G is the $(d+1)$ -dimensional Newton constant. In the limit of small total mass, we have that $B = (GM)^{-1} \ll 0$ for $M \gg 0$ which means [31, 35] that we can neglect the binding energy potential B as compared to the mass density potential Φ . One thus only needs to consider the potential Φ , i.e. Newtonian gravity.

⁴ Here we use the coordinate R which is part of the two-dimensional coordinate system $(R; \nu)$ introduced in Ref. [43] that interpolates between cylindrical coordinates $(r; z)$ and spherical coordinates $(\rho; \theta)$. In terms of $F(r; z)$ in (31) we have $R(r; z) = \sqrt{F(r; z)^2 + z^2}$. Note that Refs. [43, 31, 35] set $L = 2\pi r$, which we choose not to do here for pedagogical clarity.

For the multi-black hole configuration described above, it is not difficult to find the solution for using the method of images in terms of $(r; z)$ coordinates of the cylinder. One finds

$$\Phi(r; z) = \frac{8GM}{(d-1)L^{d-1}} F(r; z); \quad (30)$$

with

$$F(r; z) = \sum_{i=1}^m \sum_{k=1}^d \frac{x_i^k}{[r^2 + (z - z_{ij} - Lm)^2]^{\frac{d-2}{2}}}; \quad (31)$$

so that the potential (30) describes the Newtonian gravitational potential sourced by the multi-black hole configuration.

One can now study how the potential looks when going near the sources. To achieve this it is useful to define for the i^{th} black hole the spherical coordinates r and φ by

$$r = \sin \varphi; \quad z - z_i = \cos \varphi; \quad (32)$$

where φ is defined in the interval $[0; \pi]$. In terms of these coordinates one finds that $F(r; z)$ in (31) can be expanded as

$$F(\varphi; z) = \sum_i (d-2) + \sum_i^{(i)} + \sum_1^{(i)} \cos \varphi + O(\varphi^2); \quad (33)$$

for $\varphi \ll 1$, where

$$\begin{aligned} \sum_i^{(i)} &= \frac{1}{L^{d-2}} \sum_{j=1}^m \sum_{k=1}^d \frac{x_j^k}{z_{ij}^{d-2}} + (d-2; 1 - \sum_{j \neq i}^m) + (d-2; 1 + \sum_{j \neq i}^m) : \end{aligned} \quad (34)$$

Here $(s; 1+a) = \sum_{m=1}^{\infty} \frac{1}{(m+a)^s}$ is the Generalized Riemann Zeta function and z_{ij} $z_{ij}=L$ labels the distance in the z direction between the j^{th} and i^{th} black hole (see Eq. (2.24) of [35] for precise definitions).

Using now (33) with (30) one obtains the behavior of the Newtonian potential near the i^{th} black hole. This shows that the first term in (33) corresponds to the flat space gravitational potential due to the i^{th} mass $M_i = \sum_i M$ and the second term is a constant potential due to its images and the presence of the other masses and their images. The quantity $\sum_1^{(i)}$ plays a crucial role in the explicit construction of the first-order corrected metric of multi-black holes configurations on the cylinder and also enters the first-order corrected thermodynamics (see Sec. 4.2).

Equilibrium conditions. The third term in (33) is proportional to $\cos \varphi = z - z_i$ and therefore this term gives a non-zero constant term in \mathcal{O}_z if $\sum_1^{(i)}$ is non-zero. This therefore corresponds to the external force on the i^{th} black hole, due to the other $k \neq i$

black holes. Indeed, $\mathcal{F}_1^{(i)}$ can be written as a sum of the potential gradients corresponding to the gravitational force due to each of the $k-1$ other black holes on the i^{th} black hole as

$$\mathcal{F}_1^{(i)} = \sum_{j=1; j \neq i}^k V_{ij} ; \quad (35)$$

where V_{ij} corresponds to the gravitational field on the i^{th} black hole from the j^{th} black hole, given by

$$V_{ij} = \frac{(d-2)^n}{L^{d-1}} \frac{z_{ij}^{-(d-1)}}{|z_{ij}|^{d-1}} ; \quad (36)$$

for $j \neq i$. Defining $F_{ij} = -\partial_i V_{ij}$ as the Newtonian force on the i^{th} mass due to the j^{th} mass (and its images as seen in the covering space of the circle), the condition $\mathcal{F}_1^{(i)} = 0$ can be written as the condition of zero external force on each of the k masses

$$F_{ij} = 0 ; \quad (37)$$

for $i = 1, \dots, k$. As a check, note that it is not difficult to verify that Newton's law $F_{ij} = -F_{ji}$ is verified using an appropriate identity for the Generalized Zeta function (see Eq. (3.6) of [35]).

We thus conclude that for static solutions one needs to require the equilibrium condition $\mathcal{F}_1^{(i)} = 0$ for all i , since otherwise the i^{th} black hole would accelerate along the z axis. This gives conditions on the relation between the positions z_i and the mass ratios μ_i , which are examined in detail in Ref. [35]. It is shown how to build such equilibrium configurations and a general copying mechanism is described that builds new equilibrium configurations by copying any given equilibrium configuration a number of times around the cylinder.

Note that this equilibrium is an unstable equilibrium, i.e: generic small disturbances in the position of one of the black holes will disturb the balance of the configuration and result in the merger of all of the black holes into a single black hole. As also argued in Ref. [35], it is expected that these equilibrium conditions are a consequence of regularity of the solution since with a non-zero Newtonian force present on the black hole the only way to keep it static is to introduce a counter-balancing force supported by a singularity. It turns out that the irregularity of the solution cannot be seen at the leading order since the binding energy, which accounts for the self-interaction of the solution, is neglected. It is therefore expected that singularities will appear at the second order in the total mass for solutions that do not obey the equilibrium condition mentioned above.

4.2 Newtonian derivation of the thermodynamics

It turns out that there is a quick route to determine the first-order corrected thermodynamics of the multi-black hole configurations, as explained in Ref. [35] following the

method first found in Ref. [34]. Here one assumes the equilibrium condition (37) to be satisfied and all one needs is the quantity $\hat{r}_0^{(i)}$ defined in (34), i.e.: one does not need to compute the first-order corrected metric.

To start, we define for each black hole an "areal" radius $\hat{r}_0^{(i)}$, $i = 1; \dots; k$, such that the individual mass, entropy and temperature of each black hole are given by

$$M_{0(i)} = \frac{(d-1)^{d-1}}{16 G} \hat{r}_0^{(i)2d}; \quad S_{0(i)} = \frac{(d-1)^{d-1}}{4G} \hat{r}_0^{(i)d}; \quad T_{0(i)} = \frac{d-2}{4 \hat{r}_0^{(i)}}; \quad (38)$$

These are the intrinsic thermodynamic quantities associated to each black hole when they would be isolated in a flat empty $(d+1)$ -dimensional space.

If we now imagine placing the black holes on a circle at locations z_i each of them will experience a gravitational potential ϕ_i . In particular, this is the Newtonian potential created by all images of the i^{th} black hole as well as all other $k-1$ masses (and their images) as seen from the location of the i^{th} black hole. It is not difficult to show that ϕ_i is given by

$$\phi_i = -\frac{1}{2} \sum_j \frac{M_{0(j)}}{\hat{r}_i^{(j)}}; \quad (39)$$

in terms of $\hat{r}_i^{(j)}$ defined in Eq. (34). Taking into account this potential, we can now determine the thermodynamic quantities of the interacting system to leading order. By definition, the entropy $S_i = S_{0(i)}$ is unchanged. The temperature of each black hole, however, receives a redshift contribution coming from the gravitational potential ϕ_i , so that

$$T_i = T_{0(i)} (1 + \phi_i); \quad (40)$$

The total mass of the configuration is equal to the sum of the individual masses when the black holes would be isolated plus the negative gravitational (Newtonian) potential energy that appears as a consequence of the black holes and their images. We thus have that the total mass is given by

$$M = M_0 + U_{\text{Newton}}; \quad (41)$$

where

$$M_0 = \sum_{i=1}^k M_{0(i)}; \quad U_{\text{Newton}} = -\frac{1}{2} \sum_{i=1}^k \frac{M_{0(i)} \phi_i}; \quad (42)$$

From these Newtonian results one can then derive the formula for the relative tension simply by using the (generalized) first law of thermodynamics (see Eq. (6))

$$M = \sum_{i=1}^k T_i S_i + \frac{nM}{L} L; \quad (43)$$

from which one finds

$$n = \frac{L}{M} \frac{\partial M}{\partial L} \Big|_{S_i}; \quad (44)$$

The condition of keeping S_i fixed means that we should keep fixed the mass $M_{0(i)}$ of each black hole, and hence also the total intrinsic mass M_0 . It thus follows from (44) and (41) that

$$n = \frac{L}{M_0} \frac{\partial U_{\text{Newton}}}{\partial L} = \frac{1}{4M_0} \sum_{i=1}^k X_i^k M_{0(i)} \frac{\partial^{\hat{d}-2}}{\partial L^{(i)}} \frac{\partial}{\partial L} = \frac{d-2}{4} \sum_{i=1}^k X_i^k \frac{\partial^{\hat{d}-2}}{\partial L^{(i)}}; \quad (45)$$

where we used that $\partial^{\hat{d}-2} / \partial L^{(d-2)}$ for fixed locations z_i (see Eq. (34)) and $M_{0(i)} = z_i M_0$. As shown in [35], the thermodynamics above agrees with the explicitly computed thermodynamic quantities from the first-order corrected metric.

We emphasize that these results are correct only to first order in the mass and note that in terms of the reduced mass (7) the expression (45) gives that n as a function of μ is given for the multi-black hole configurations by

$$n(\mu) = \frac{(d-2)(2)^{\hat{d}-2}}{4(d-1)^{\hat{d}-1}} \sum_{i=1}^k X_i^k \mu^{(i)} + O(\mu^2); \quad (46)$$

which generalizes the single-black hole result given in (17). In terms of the phase diagram of Fig. 1, it follows from this result that (at least for small masses) the k black hole configurations correspond to points lying above the single-black hole phase and below the k copied phase.

From the first-order corrected temperatures (40) one can show that the multi-black hole configurations are in general not in thermal equilibrium. The only configurations that are in thermal equilibrium to this order are the copies of the single-black hole solution studied previously [98, 52, 31]. As a further comment we note that Hawking radiation will seed the mechanical instabilities of the multi-black hole configurations. The reason for this is that in a generic configuration the black holes have different rates of energy loss and hence the mass ratios required for mechanical equilibrium are not maintained. This happens even in special configurations, e.g: when the temperatures are equal, because the thermal radiation is only statistically uniform. Hence asymmetries in the real time emission process will introduce disturbances driving these special configurations away from their equilibrium positions.

4.3 Consequences for the phase diagram

The existence of the multi-black hole solutions has striking consequences for the phase structure of black hole solutions on $M^{\hat{d}} \times S^1$. It means that one can for example start from a solution with two equal size black holes, placed oppositely to each other on the cylinder, and then continuously deform the solution to be arbitrarily close to a solution with only one black hole (the other black hole being arbitrarily small in comparison). Thus, we get a continuous span of classical static solutions for a given total mass. In particular, a multi-black hole configuration with k black holes has k independent parameters. This implies a continuous non-uniqueness in the $(\mu; n)$ phase diagram (or for a given mass),

much like the one observed for bubble-black hole sequences [49] and for other classes of black hole solutions [99, 17, 19, 18] (see also Sec. 6). In particular, this has the consequence that if we would live on $M^4 \times S^1$ then from a four-dimensional point of view one would have an infinite non-uniqueness for static black holes of size similar to the size of the extra dimension, thus severely breaking the uniqueness of the Schwarzschild black hole.

New non-uniform strings? Another consequence of the new multi-black hole configurations is for the connection to uniform and non-uniform strings on the cylinder. As discussed in Sec. 3.3, there is evidence that the black hole on the cylinder phase merges with the non-uniform black string phase in a topology changing transition point. It follows from this that the copies of black hole on the cylinder solution merge with the copies of non-uniform black strings. However, due to the multi-black hole configurations we now have a continuous span of solutions connected to the copies of the black hole on the cylinder. Therefore, it is natural to ask whether the new solutions also merge with non-uniform black string solutions in a topology changing transition point. If so, it probes the question whether there exist, in addition to having new black hole on the cylinder solutions, also new non-uniform black string solutions. Thus, these new solutions present a challenge for the current understanding of the phase diagram for black holes and strings on the cylinder. For a detailed discussion on this see Ref. [35].

Another connection with strings and black holes on the cylinder is that a Gregory-Laflamme unstable uniform black string is believed to decay to a black hole on the cylinder (when the number of dimensions is less than the critical one [39]). However, the new multi-black hole solutions mean that one can imagine them as intermediate steps in the decay.

Lumpy black holes. Ref. [35] also examines in detail configurations with two and three black holes. For two black holes this confirms the expectation that one maximizes the entropy by transferring all the mass to one of the black holes, and also that if the two black holes are not in mechanical equilibrium then the entropy is increasing as the black holes become closer to each other. These two facts are both in accordance with the general argument that the multi-black hole configurations are in an unstable equilibrium and generic perturbations of one of the positions will result in that all the black holes merge together in a single black hole on the cylinder.

A detailed examination of the three black hole solution suggests the possibility of further new types of black hole solutions in Kaluza-Klein spacetimes. In particular, this analysis suggests the possibility that new static configurations may exist that consist of a lumpy black hole, where the non-uniformities are supported by the gravitational stresses imposed by an external field. These new solutions were argued by considering a symmetric configuration of three black holes, with one of mass M_1 and two others of equal mass $M_2 = M_3$ at equal distance to the first one. Increasing the total mass of the system shows that it is possible that the two black holes (2 and 3) merge before merging with black hole 1. In this way one could end up with a static solution consisting of lumpy black hole (i.e.

a ‘peanut-like’ shaped black object) together with an ellipsoidal black hole.

An analogue fluid model. Finally we note that one may consider the multi-black hole configurations in relation to an analogue fluid model for the Gregory-Laammé (GL) instability, recently proposed in Ref. [90]. There it was pointed out that the GL instability of a black string has a natural analogue description in terms of the Rayleigh-Plateau (RP) instability of a fluid cylinder. It turns out that many known properties of the gravitational instability have an analogous manifestation in the fluid model. These include the behavior of the threshold mode with d , dispersion relations, the existence of critical dimensions and the initial stages of the time evolution (see Refs. [90, 91, 100] for details). In the context of this analogue fluid model, Ref. [35] discusses a possible, but more speculative, relation of the multi-black hole configurations to configurations observed in the time evolution of fluid cylinders.

5 Thin black rings in higher dimensions

In this and the next section we turn our attention to rotating black holes. We start by reviewing the recent construction [30] of an approximate solution for an asymptotically flat neutral thin rotating black ring in any dimension $D \geq 5$ with horizon topology $S^{D-3} \times S^1$. As in Sec. 4, this construction uses the method of matched asymptotic expansion, and we only present the main points. We discuss in particular the equilibrium condition necessary for balancing the ring, and how this enables to obtain the leading order thermodynamics of thin rotating black rings. We also compare the thermodynamics of the thin black ring to that of the MP black hole. In this and the following section we denote the number of spacetime dimensions by $D = 4 + n$.

5.1 Thin black rings from boosted black strings

Black rings in $(n + 4)$ -dimensional asymptotically flat spacetime are solutions of Einstein gravity with an event horizon of topology $S^1 \times S^{n+1}$. As we briefly reviewed in Secs. 1 and 2 explicit solutions with this topology in five dimensions ($n = 1$) were first presented in Ref. [16] (see also [2] for a review).

In five dimensions, there is beyond the MP black hole and the black ring one more phase of rotating black holes if one restricts to phases with a single angular momentum that are in thermal equilibrium. This is the black Saturn phase consisting of a central MP black and one black ring around it, having equal temperature and angular velocity. If one abandons the condition of thermal equilibrium there are many more black Saturn phases with multiple rings as well as multi-black ring solutions. We refer to [18] and the recent review [4] for details on the more general phase structure for the five-dimensional case.

The construction of analogous solutions in more than five dimensions is considerably more involved, since for $D \geq 6$ these solutions are not contained in the generalized Weyl

ansatz [24, 25, 101] because they do not have $D = 2$ commuting Killing symmetries. Furthermore the inverse scattering techniques of [26, 27, 28, 29] do not extend to the asymptotically flat case in any $D \geq 6$.

Therefore, one way to make progress towards solving this problem can be achieved by first constructing thin black ring solutions in arbitrary dimensions as a perturbative expansion around circular boosted black strings. The idea that rotating thin black rings should be well approximated by boosted black strings is intuitively clear and already appears in earlier works [102, 103, 104]. This was used as a starting point in the explicit construction [30].

Boosted black string. The zeroth order solution is that of a straight boosted black string. The metric of this can easily be obtained from (11) by applying a boost in the $(t; z)$ plane. The result is

$$ds^2 = - \left(1 - \cosh^2 \frac{r_0^n}{r^n} \right) dt^2 - 2 \frac{r_0^n}{r^n} \cosh \sinh dt dz + \left(1 + \sinh^2 \frac{r_0^n}{r^n} \right) dz^2 + \left(1 - \frac{r_0^n}{r^n} \right) dr^2 + r^2 d\Omega_{n+1}^2; \quad (47)$$

where r_0 is the horizon radius and β is the boost parameter. In general, we will take the z direction to be along an S^1 with circumference $2\pi R$, which means we can write z in terms of an angular coordinate defined by $z = R\phi$ ($0 \leq \phi < 2\pi$). At distances $r \gg R$, the solution (47) is the approximate metric of a thin black ring to zeroth order in $1/R$.

By definition, a thin black ring has an S^1 radius R that is much larger than its S^{n+1} radius r_0 . In this limit, the mass of the black ring is small and the gravitational attraction between diametrically opposite points of the ring is very weak. So, in regions away from the black ring, the linearized approximation to gravity will be valid, and the metric will be well-approximated if we substitute the ring by an appropriate delta-like distributional source of energy-momentum. The source has to be chosen so that the metric it produces is the same as that expected from the full exact solution in the region far away from the ring. Since the thin black ring is expected to approach locally the solution for a boosted black string, it is sensible to choose distributional sources that reproduce the metric (47) in the weak-field regime,

$$T_{tt} = \frac{r_0^n}{16 G} \left(n \cosh^2 \frac{r_0^n}{r^n} + 1 \right) \delta^{(n+2)}(r); \quad (48a)$$

$$T_{tz} = \frac{r_0^n}{16 G} n \cosh \sinh \frac{r_0^n}{r^n} \delta^{(n+2)}(r); \quad (48b)$$

$$T_{zz} = \frac{r_0^n}{16 G} \left(n \sinh^2 \frac{r_0^n}{r^n} - 1 \right) \delta^{(n+2)}(r); \quad (48c)$$

The location $r = r_0$ corresponds to a circle of radius R in the $(n+3)$ -dimensional Euclidean space, parameterized by the angular coordinate ϕ . In this construction the mass and angular momentum of the black ring are obtained by integrating the energy and

momentum densities,

$$M = 2 R \int_{S^{n+1}} T_{tt} ; J = 2 R^2 \int_{S^{n+1}} T_{tz} ; \quad (49)$$

where S^{n+1} links the ring once.

Dynamical equilibrium condition. We now first show that the boost parameter gets fixed by a dynamical equilibrium condition ensuring that the string tension is balanced against the centrifugal repulsion. To this end note that we are approximating the black ring by a distributional source of energy-momentum. The general form of the equation of motion for probe brane-like objects in the absence of external forces takes the form [105]

$$K_{\alpha\beta} - T_{\alpha\beta} = 0 ; \quad (50)$$

where the indices α, β are tangent to the brane and z is transverse to it. The second fundamental tensor $K_{\alpha\beta}$ extends the notion of extrinsic curvature to submanifolds of codimension possibly larger than one. The extrinsic curvature of the circle is $1/R$, so a circular linear distribution of energy-momentum of radius R will be in equilibrium only if

$$\frac{T_{zz}}{R} = 0 ; \quad (51)$$

ie: for finite radius the pressure tangential to the circle must vanish. Hence, for the thin black ring with source (48), the condition that the ring be in equilibrium translates into a very specific value for the boost parameter

$$\sinh^2 \alpha = \frac{1}{n} ; \quad (52)$$

which we will also refer to as the critical boost. For $D = 5$ ($n = 1$) this was already observed in Ref. [102] where the thin black string limit of five-dimensional black rings was first made explicit, but the connection with (50) was first noticed in [30].

Thermodynamics. Using (52) it is not difficult to obtain the physical quantities of the critically boosted black string, and hence the leading-order thermodynamics of thin black rings (see also Refs. [103, 106] for further details on boosted black strings and their thermodynamics). We end for the mass M , entropy S , temperature T , angular momentum J and angular velocity the expressions [30]

$$M = \frac{n+1}{8G} R r_0^n (n+2) ; S = \frac{n+1}{2G} R r_0^{n+1} \frac{r_0}{n} ; T = \frac{n}{4} \frac{r_0}{n+1} \frac{1}{r_0} ; \quad (53a)$$

$$J = \frac{n+1}{8G} R^2 r_0^n \frac{1}{n+1} ; \quad \Omega = \frac{1}{n+1} \frac{1}{R} ; \quad (53b)$$

We also note that an equivalent but more physical form of the equilibrium equation (52) in terms of these quantities is

$$R = \frac{n+2}{n+1} \frac{J}{M} ; \quad (54)$$

We thus see that the radius grows linearly with J for fixed mass.

It is remarkable that with the above reasoning one can already obtain the correct limiting thermodynamics of thin black rings to leading order, without having to solve for any metric. One finds from (53) that the entropy of thin black rings behaves as

$$S^{\text{ring}}(M; J) / J^{\frac{1}{D-4}} M^{\frac{D-2}{D-4}}; \quad (55)$$

whereas that of ultra-spinning MP black holes in $D = 6$ is given by [6]

$$S^{\text{hole}}(M; J) / J^{\frac{2}{D-5}} M^{\frac{D-2}{D-5}}; \quad (56)$$

This already shows the non-trivial fact that in the ultra-spinning regime of large J for fixed mass M the rotating black ring has higher entropy than the MP black hole (see also Sec. 5.3). Moreover, as will be explained in Sec. 5.2, it turns out that for $D = 6$ the results (53) are actually valid up to and including the next order in $r_0=R$, so receives only $O(r_0^2=R^2)$ corrections. This conclusion could already be drawn once one has convinced oneself that the first-order $l=R$ correction terms in the metric only involve dipole contributions which can easily be argued to give zero contribution to all thermodynamic quantities [30].

It is important to stress that the above reasoning relies crucially on the assumption that when the boosted black string is curved, the horizon remains regular. To verify this point, and also to obtain a metric for the thin black ring, Ref. [30] solves the Einstein equations explicitly by constructing an approximate solution for $r_0 \ll R$ using a matched asymptotic expansion. In this analysis one finds that the condition (51) appears as a consequence of demanding absence of singularities on the plane of the ring outside the horizon. Whenever $n \sinh^2 \epsilon \ll 1$ with finite R , the geometry backreacts creating singularities on the plane of the ring. These singularities admit a natural interpretation. Since (50) is a consequence of the conservation of the energy-momentum tensor, when (51) is not satisfied there must be additional sources of energy-momentum. These additional sources are responsible for the singularities in the geometry. Alternatively, the derivation of (51) in Ref. [30] from the Einstein equations is an example of how General Relativity encodes the equations of motion of black holes as regularity conditions on the geometry.

5.2 Matched asymptotic expansion

We now review the highlights of the perturbative construction of thin black rings using matched asymptotic expansion (see also Sec. 4.1). In the problem at hand, the two widely separated scales are the ‘thickness’ of the ring r_0 and the radius of the ring R , and the thin limit means that $r_0 \ll R$. There are therefore two zones, an asymptotic zone at large distances from the black ring, $r \gg r_0$, where the field can be expanded in powers of r_0 . The other zone is the near-horizon zone which lies at scales much smaller than the ring radius, $r \ll R$. In this zone the field is expanded in powers of $l=R$. At each step, the

solution in one of the zones is used to provide boundary conditions for the field in the other zone, by matching the fields in the ‘overlap’ zone $r_0 < r < R$ where both expansions are valid.

As already discussed in Sec. 5.1, the starting point is to consider the solution in the near-horizon zone to zeroth order in $1=R$, i.e: we take a boosted black string of infinite length, $R \gg 1$. The next steps in the construction are then as follows:

Step 1: One solves the Einstein equations in the linearized approximation around flat space for a source corresponding to a circular distribution of a given mass and momentum density as given in (48). This metric is valid in the region $r < r_0$.

Step 2: We consider the Newtonian solution close to the sources, i.e: in the overlap region $r_0 < r < R$.

Step 3: We consider the near-horizon region of the ring and find the linear corrections to the metric of a boosted black string for a perturbation that is small in $1=R$; in other words, we analyze the geometry of a boosted black string that is now slightly curved into a circular shape. This solution is then matched to the metric in the overlap region found in Step 2. The resulting solution is valid in the region $r_0 < r < L$.

To solve Step 1 for a non-zero $T_{zz} = R^2 T_{zz}$ is not easy. It is therefore convenient to already assume that the equilibrium condition $T_{zz} = 0$ in (51) is satisfied. This then gives the solution of a black ring in linearized gravity [30]. Finding a more general solution with a source for the tension is much easier if one restricts to the overlap zone (Step 2). In this regime we are studying the effects of locally curving a thin black string into an arc of constant curvature radius R . To this end it is convenient to introduce ring-adapted coordinates. These are derived in Ref. [30] and to first-order in $1=R$ the flat space metric in these coordinates takes the form

$$ds^2(\mathbb{E}^{n+3}) = \left(1 + \frac{2r \cos \theta}{R}\right) dz^2 + \left(1 - \frac{2r \cos \theta}{R}\right) dr^2 + r^2 d\theta^2 + r^2 \sin^2 \theta d\Omega_n^2 : \quad (57)$$

In terms of these coordinates the general form of the metric in the overlap region is then

$$g_{\mu\nu} = g_{\mu\nu}^{(0)} + \frac{r_0^n}{r^n} h^{(0)}(r) + \frac{r \cos \theta}{R} h^{(1)}(r) : \quad (58)$$

Solving Einstein equations to order $1=R$ then explicitly shows that regularity of the solution enforces vanishing of the tension T_{zz} (see Eq. (51)).

The technically most difficult part of the problem is to find the near-horizon solution in step 3. Physically, this corresponds to curving the black string into a circle of large but finite radius R . In effect, this means that we are placing the black string in an external potential whose form at large distances is that of (58) and which changes the metric g^{bbs} in Eq. (47) of the (critically) boosted black string by a small amount, i.e: .

$$g_{\mu\nu} = g^{\text{bbs}}(r; r_0) + \frac{\cos \theta}{R} h_{\mu\nu}(r; r_0) : \quad (59)$$

In Ref. [30] the Einstein equations to order $l=R$ are explicitly solved, showing that the perturbations $h_{\mu\nu}(r; r_0)$ can be expressed in terms of hypergeometric functions.

Corrected thermodynamics. One can find the corrections to the thermodynamics as follows. First, one uses the near-horizon corrected metric (59) to find the corrections to the entropy S , temperature T , and angular velocity J . Then one can use the 1st law,

$$dM = T dS + J dJ; \quad (60)$$

and the Smarr formula

$$(n+1)M = (n+2)(TS + J); \quad (61)$$

to deduce the corrections to the mass and angular momentum.⁵ Using now that the perturbations in (59) are only of dipole type, with no monopole terms, it follows that the area, surface gravity and angular velocity receive no modifications in $l=R$. The reason is that a dipole can not change the total area of the horizon, only its shape. This is true both of the shape of the S^{n+1} as well as the length of the S^1 , which can vary with r but on average (i.e: when integrated over the horizon) remains constant. So S is not corrected. The surface gravity and angular velocity can not be corrected either. They must remain uniform on a regular horizon, so, since the dipole terms vanish at $l=R-2$, no corrections to T and J are possible. It then follows from (60), (61) that M and J are not corrected either.⁶ So the function $S(M; J)$ obtained in (55) is indeed valid including the first order in $l=R$. It is interesting to observe that this conclusion could be drawn already when the asymptotic form of the metric (58) in the overlap zone, is seen to include only dipole terms at order $l=R$.

5.3 Black rings versus MP black holes

We now proceed by analyzing the thin black ring thermodynamics and compare it to that of ultra-spinning MP black holes. Recall that the thermodynamics of the thin black ring in the ultra-spinning regime is given by (53), which is valid up to $O(r_0^2=R^2)$ corrections.

Meyers-Perry black hole. For the MP black hole, exact results can be obtained for all values of the rotation. The two independent parameters specifying the (single-angular momentum) solution are the mass parameter m and the rotation parameter a , from which the horizon radius r_0 is found as the largest (real) root of the equation

$$r_0^{2n} = (r_0^2 + a^2)r_0^{n-1}; \quad (62)$$

In terms of these parameters the thermodynamics take the form [15]

$$M = \frac{(n+2)r_0^{n+2}}{16G}; \quad S = \frac{n+2}{4G} r_0; \quad T = \frac{1}{4} \left(\frac{2r_0^n}{r_0} + \frac{n-1}{r_0} \right); \quad (63a)$$

⁵This method was also used in Ref. [31, 35] for small black holes and multi-black holes on the cylinder.

⁶In d -dimensions ($n = d-1$) there are corrections to this order. Their origin is discussed in App. A of [30].

$$J = \frac{n+2}{8} \frac{a}{G}; \quad = \frac{a r_0^{n-1}}{8 G}; \quad (63b)$$

Note the similarity between $a = \frac{n+2}{2} \frac{J}{M}$ and the black ring relation (54).

An important simplification occurs in the ultra-spinning regime of $J \ll 1$ with fixed M , which corresponds to $a \ll 1$. Then (62) becomes $\approx a^2 r_0^{n-1}$ leading to simple expressions for Eq. (63) in terms of r_0 and a , which in this regime play roles analogous to those of r_0 and R for the black ring. Specifically, a is a measure of the size of the horizon along the rotation plane and r_0 a measure of the size transverse to this plane [36]. In fact, in this limit

$$M \approx \frac{(n+2)}{16} \frac{n+2}{G} a^2 r_0^{n-1}; \quad S \approx \frac{n+2}{4G} a^2 r_0^n; \quad T \approx \frac{n}{4} \frac{1}{r_0}; \quad (64)$$

take the same form as the expressions characterizing a black membrane extended along an area a^2 with horizon radius r_0 . This identification lies at the core of the ideas in [36], which were further developed in Ref. [30] and will be summarized in Sec. 6. We note that the quantities J and Ω disappear since the black membrane limit is approached in the region near the axis of rotation of the horizon and so the membrane is static in the limit. Note furthermore that (64) is valid up to $O(r_0^2 = a^2)$ corrections.

Finally, we remark that the transition to the membrane-like regime is signaled by a qualitative change in the thermodynamics of the MP black holes. At $a=r_0 = \frac{1}{2} \left(\frac{n+1}{n-1} \right)^{1/n}$ the temperature reaches a minimum and $\partial^2 S = \partial J^2_M$ changes sign. For $a=r_0$ smaller than this value, the thermodynamic quantities of the MP black holes such as T and S behave similarly to those of the Kerr solution and one should not expect any membrane-like behavior. However, past this point they rapidly approach the membrane results. We do not expect that the onset of thermodynamic instability at this point is directly associated to any dynamical instability. Rather, one expects a GL-like instability to happen at a larger value of $a=r_0$ [36, 30].

Dimensionless quantities. Contrary to the case of KK black holes where we could use the circle length to define dimensionless quantities (cf. (7) or (8)) in this case we need to use one of the physical parameters of the solutions to define dimensionless quantities. We choose the mass M and thus introduce dimensionless quantities for the spin j , the area a_H , the angular velocity Ω_H and the temperature t_H via

$$j^{n+1} / \frac{J^{n+1}}{GM^{n+2}}; \quad a_H^{n+1} / \frac{S^{n+1}}{(GM)^{n+2}}; \quad (65a)$$

$$\Omega_H / (GM)^{\frac{1}{n+1}}; \quad t_H / (GM)^{\frac{1}{n+1}} T; \quad (65b)$$

where convenient normalization factors can be found in Eq. (7.9) of [30]. We take j as our control parameter and now study and compare the functions $a_H(j)$, $\Omega_H(j)$ and $t_H(j)$ for black rings and MP black holes in the ultra-spinning regime. These asymptotic

phase curves can now be obtained using (65) together with (53) and (64) respectively. In the following we denote the results for the thin black ring with (r) and for the ultra-spinning MP black holes with (h) , and generally omit numerical prefactors.

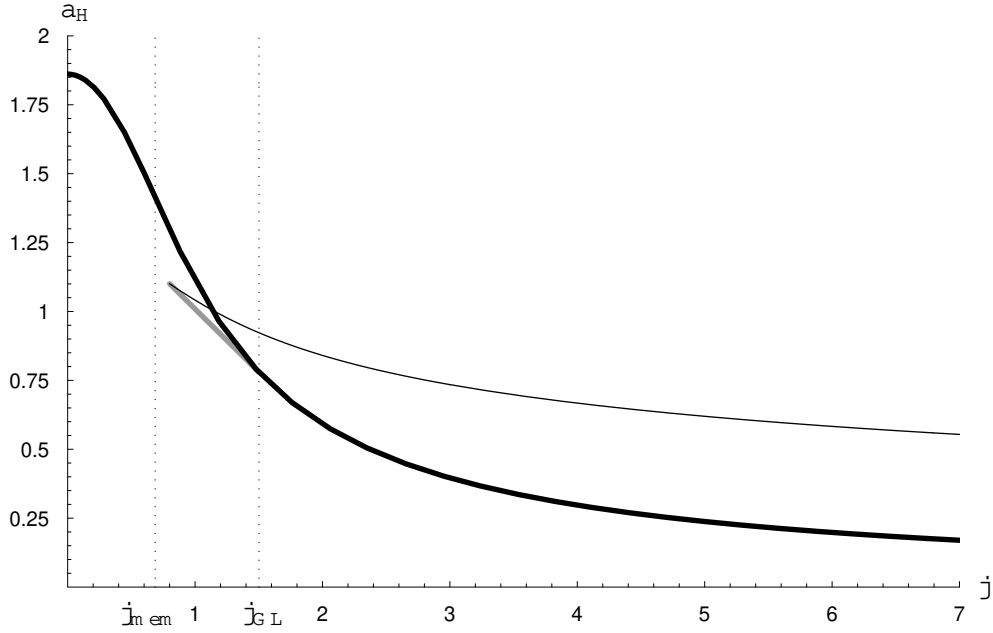


Figure 3: Area vs spin for fixed mass, $a_H(j)$, in seven dimensions. For large j , the thin curve is the result for thin black rings and is extrapolated here down to $j \rightarrow 0$ (1). The thick curve is the exact result for the MP black hole. The gray line corresponds to the conjectured phase of pinched black holes (see Sec. 6), which branches off tangentially from the MP curve at a value $j_{GL} > j_{mem}$. At any given dimension, the phases should not necessarily display the swallowtail as shown in this diagram, but could also connect more smoothly via a pinched black hole phase that starts tangentially in j_{GL} and has increasing j . Reprinted from Ref. [30].

Comparison of the thermodynamics. Starting with the reduced area function we see that

$$a_H^{(r)} \sim \frac{1}{j^{1-n}}; \quad a_H^{(h)} \sim \frac{1}{j^{2-(n-1)}}; \quad (66)$$

and so, for any $D = 4 + n \geq 6$, the area decreases faster for MP black holes than for black rings, so we immediately see that black rings dominate entropically in the ultra-spinning regime [30]. For illustration, Fig. 3 shows these curves in $D = 7$ ($n = 3$).

Including prefactors one finds for the angular velocities that

$$\omega_H^{(r)} \sim \frac{1}{2j}; \quad \omega_H^{(h)} \sim \frac{1}{j}; \quad (67)$$

The ratio $\omega_H^{(h)} / \omega_H^{(r)} = 2$, which holds for all $D \geq 6$, is reminiscent of the factor of 2 in Newtonian mechanics between the moment of inertia of a wheel (i.e. a ring) and a disk (i.e. a pancake) of the same mass and radius, which implies that the disk must rotate twice as fast as the wheel in order to have the same angular momentum. Irrespective of

whether this is an exact analogy or not, the fact that $!_H^{(r)} < !_H^{(h)}$ is clearly expected from this sort of picture. For the temperatures we find

$$t_H^{(r)} \propto j^{j=n}; \quad t_H^{(h)} \propto j^{j=(n-1)}; \quad (68)$$

so the thin black ring is colder than the M P black hole. In fact, since the temperature is inversely proportional to the thickness of the object the picture suggested above leads to the following argument: if we put a given mass in the shape of a wheel of given radius, then we get a thicker object than if we put it in the shape of a pancake of the same radius.

6 Completing the phase diagram

In this section we will discuss the phase structure of asymptotically flat neutral rotating black holes in six and higher dimensions by exploiting a connection between, on one side, black holes and black branes in KK spacetimes and, on the other side, higher-dimensional rotating black holes. Building on the basic idea in [36], this phase structure was recently proposed in Ref. [30]. Part of this picture is conjectural, but is based on well-motivated analogies and appears to be natural from many points.

The curve $a_H(j)$ at values of j outside the domain of validity of the computations in Sec. 5 corresponds to the regime where the gravitational self-attraction of the ring is important. There are no analytical methods presently known to treat such values $j \gg 0(1)$, and the precise form of the curve in this regime may require numerical solutions. However, as argued in Ref. [30] it is possible to complete the black ring curve and other features of the phase diagram, at least qualitatively. This is done by combining a number of observations and reasonable conjectures about the behavior of M P black holes at large rotation and using as input the presently known phase structure of Kaluza-Klein black holes (see Sec. 3).

6.1 GL instability of ultra-spinning M P black hole

In the ultra-spinning regime in $D = 6$, M P black holes approach the geometry of a black membrane $R^2 \times S^{D-4}$ spread out along the plane of rotation [36]. In Sec. 5.3 we have already observed that the extent of the black hole along the plane is approximately given by the rotation parameter a , while the ‘thickness’ of the membrane, i.e. the size of its S^{D-4} , is given by the parameter r_0 . For $a=r_0$ larger than a critical value of order one we expect that the dynamics of these black holes is well-approximated by a black membrane compactified on a square torus T^2 with side length $L = a$ and with S^{D-4} size r_0 . The angular velocity of the black hole is always moderate, so it will not introduce large quantitative differences, but note that the rotational axial symmetry of the M P black holes translates into only one translational symmetry along the T^2 , the other one being broken.

Using this analogy mapping of membranes and fastly rotating M P black holes, Ref. [36] argued that the latter should exhibit a Gregory-Laam-type instability. Furthermore,

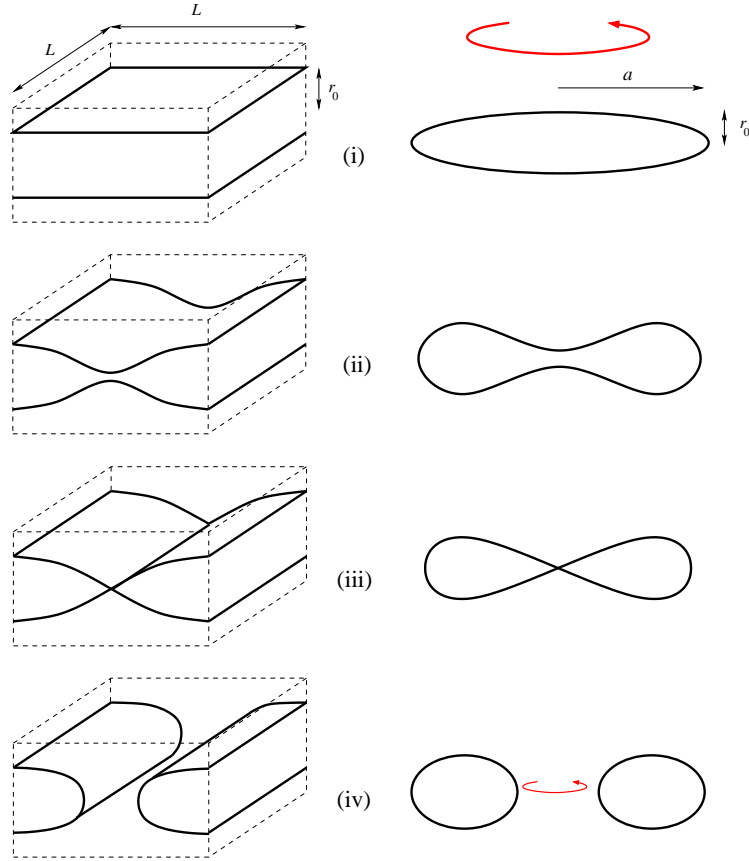


Figure 4: Correspondence between phases of black membranes wrapped on a T^2 of side L (left) and fast-rotating MP black holes with rotation parameter $a = L/r_0$ (right; must be rotated along a vertical axis): (i) Uniform black membrane and MP black hole. (ii) Non-uniform black membrane and pinched black hole. (iii) Pinched-off membrane and black hole. (iv) Localized black string and black ring. Reprinted from Ref. [30].

as reviewed in Sec. 3 it is known that the threshold mode of the GL instability gives rise to a new branch of static non-uniform black strings and branes [92, 37, 38]. In correspondence with this, Ref. [36] argued that it is natural to conjecture the existence of new branches of axisymmetric ‘lumpy’ (or ‘pinched’) black holes, branching off from the MP solutions along the stationary axisymmetric zero-mode perturbation of the GL-like instability,

Map to phases of KK black holes on the torus. In Ref. [30] this analogy was pushed further by drawing a correspondence between the phases of KK black holes on the torus (see Sec. 3.4) and the phases of higher-dimensional black holes, as illustrated in Fig. 4. Here we have restricted to non-uniformities of the membrane along only of the two brane directions, since including non-uniformity in a second direction would not have a counterpart for rotating black holes. These would break axial symmetry and hence would be radiated away. Other limitations of the analogy are discussed in detail in Ref. [30].

Using the correspondence between the phases of the two systems, one can import, at

least qualitatively, the known phase diagram of black membranes on $M^{D-2} \times T^2$ onto the phase diagram of rotating black objects in M^D . To this end one needs to first establish the map between quantities on each side of this correspondence. For unit mass, the quantities ℓ (see Eq. (8)) and j (see Eq. (65)) measure the (linear) size of the horizon along the torus or rotation plane, respectively. Then $a_H(\ell)$ for KK black holes on $M^{n+2} \times T^2$ is analogous (up to constants) to $a_H(j)$ for rotating black holes in M^{n+4} .

More precisely, although the normalization of magnitudes in (65) and (8) are different, the functional dependence of a_H on ℓ or j must be parametrically the same in both functions, at least in the regime where the analogy is precise. As a check on this, note that the function $a_H(\ell)$ in (23) for the uniform black membrane exhibits exactly the same functional form (66) as $a_H(j)$ for the MP black hole in the ultra-spinning limit. Similarly, (24) for the localized black string shows the same functional form as (66) for the black ring in the large j limit. The most important application of the analogy, though, is to non-uniform membrane phases (see Eq. (25)), providing information about the phases of pinched rotating black holes and how they connect to MP black holes and black rings.

6.2 Phase diagram of neutral rotating black holes on M^D

We present here the main points of the proposed phase diagram [30] of neutral rotating black holes (with one angular momentum) in asymptotically flat space that follows from the analogy described above. To this end, we recall that the phases of KK black holes on a two-torus were discussed in Sec. 3.4 and depicted in the representative phase diagram Fig. 2.

Main sequence. The analogy developed above suggests that the phase diagram of rotating black holes in the range $j > j_{\text{mem}}$ where MP black holes behave like black membranes, is qualitatively the same as that for KK black holes on the torus (see Fig. 2), with a pinched (lumpy) rotating black hole connecting the MP black hole with the black ring. This phase is depicted in Fig. 3 as a gray line emerging tangentially from the MP black hole curve at a critical value j_{GL} that is currently unknown. Arguments were given in [36] to the effect that $j_{\text{GL}} > j_{\text{mem}}$, consistent with the analogy. As one moves along the gray line in Fig. 3 in the direction away from the MP curve, the pinch at the rotation axis of these black holes grows deeper. Eventually, as depicted in Fig. 4, the horizon pinches down to zero thickness at the axis and then the solutions connect to the black ring phase. Note also that we may have the ‘swallow tail’ structure of first-order phase transitions (as depicted Fig. 3), or instead that of second-order phase transitions (see Fig. 4 of [30]). It may not be unreasonable to expect that a swallow tail appears at least for the lowest dimensions $D = 6; 7; \dots$, since this is in fact the same type of phase structure that appears for $D = 5$.

Beyond this main sequence, Ref. [30] presents arguments for further completion of the phase diagram, which is summarized in Fig. 5. The most important features are as follows.

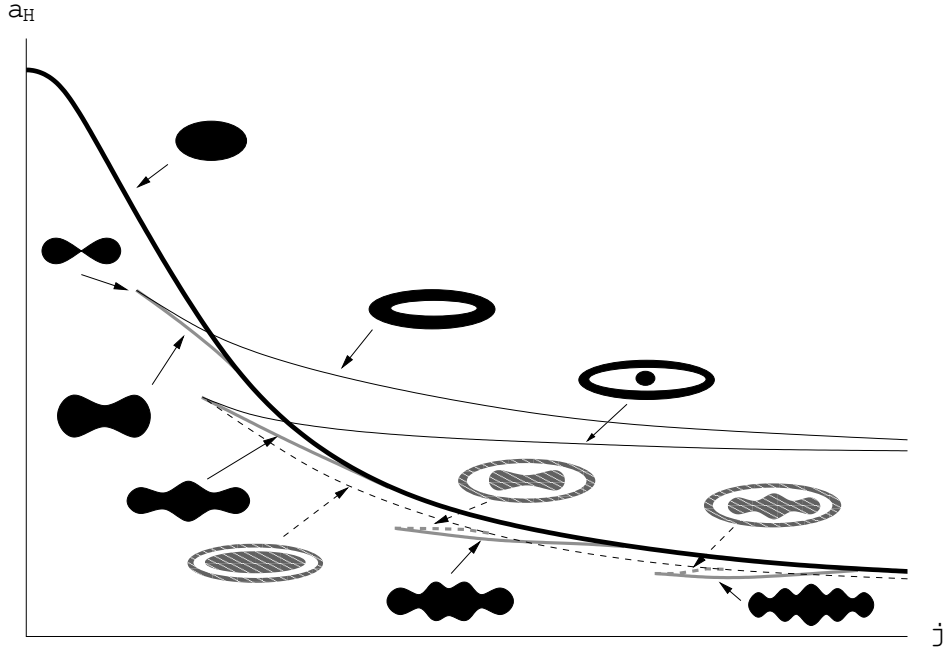


Figure 5: Proposal for the phase diagram of the all equilibrium phases of rotating black holes in $D = 6$ with one angular momentum. The solid lines and figures have significant arguments in their favor, while the dashed lines and figures might not exist and admit conceivable, but more complicated, alternatives. Some features have been drawn arbitrarily, e.g.: at any given bifurcation and in any dimension one may either have smooth connections or swallow tails with cusps. If thermalequilibrium is not imposed, the whole semi-infinite strip $0 < a_H < a_H(j=0), 0 < j < 1$ is covered, and multi-rings are possible. Reprinted from Ref. [30].

Infinite sequence of lumpy (pinched) black holes. Another observation based on the membrane analogy is that the phase diagram of rotating black holes should also exhibit an infinite sequence [36, 30] of lumpy (pinched) black holes emerging from the curve of MP black holes at increasing values of j . These are the analogues of the k -copied phases in the phase diagram of KK black holes that appear at increasing λ according to (26). In this connection note that for the GL zero-modes of MP black holes one must choose axially-symmetric combinations, implying a change of basis from plane waves $\exp(ik_{GL}z)$ to Bessel functions. Axially symmetric modes have a profile $J_0(k_{GL}a \sin \theta)$ [36]. The main point here is that the wavelength λ_{GL} (see (15)) of the GL zero-mode remains the same in the two analogue systems, to first approximation, even if the profiles are not the same. One is thus led to the existence of an infinite sequence of pinched black hole phases emanating from the MP curve at increasing values $j_{GL}^{(k)}$.

Black Saturn. If we focus on the first copy ($k = 2$), on the KK black hole side this corresponds to a non-uniform membrane on T^2 with a GL zero-mode perturbation of the membrane with two minima, which grows to merge with a configuration of two identical black strings localized on the torus. For the MP black hole, the analogue is the development of a circular pinch, which then grows deeper until the merger with a black Saturn

configuration in thermal equilibrium. Thermal equilibrium, i.e.: equal temperature and angular velocity on all disconnected components of the event horizon, is in fact naturally expected for solutions that merge with pinched black holes, since the temperature and angular velocity of the latter should be uniform on the horizon all the way down to the merger, and we do not expect them to jump discontinuously there. These appear to be the natural higher-dimensional generalization of the *ve*-dimensional black Saturn [17], and one may invoke the same arguments as those in Ref. [18]. When the size of the central black hole is small compared to the radius of the black ring, the interaction between the two objects is small and, to a first approximation, one can simply combine them linearly. It follows that, under the assumption of equal temperatures and angular velocities for the two black objects in the black Saturn, as j is increased a larger fraction of the total mass and the total angular momentum is carried by the black ring, and less by the central black hole. Then, this black Saturn curve must asymptote to the curve of a single black ring.

Pancaked and pinched black Saturns. The existence of these phases and their appearance in the phase diagram Fig. 5 (in which they appear dashed) is based on comparatively less compelling arguments. Nevertheless, these conjectural phases provide a simple and natural way of completing the curves in the phase diagram that is consistent with the available information. We refer to Ref. [30] for further details on these phases.

It should also be noted that in the diagram of Fig. 5 only the thermal equilibrium phases among the possible multi-black hole phases are represented. The existence of multi-black rings, with or without a central black hole, in thermal equilibrium is not expected. In general one does expect the existence of multi-black ring configurations, possibly with a central black hole, in which the different black objects have different surface gravities and different angular velocities. These configurations can be seen as the analogue of the multi-localized string configurations on the torus that can be obtained from multi-black hole configurations on the circle [35] discussed in Sec. 4 by adding a uniform direction.

7 Outlook

We conclude by briefly presenting a number of important issues and questions for future research. See also the reviews [1, 2, 3, 4] for further discussion and other open problems.

Stability. In both classes discussed in this lecture it would be interesting to further study the stability of the various solutions. For KK black holes, this includes the classical stability of the non-uniform black string and the localized black hole. For the rotating black hole case, we note that black rings at large j in any $D \geq 5$ are expected to suffer from a GL instability that creates ripples along the S^1 and presumably fragments the black ring into black holes flying apart [16, 103, 104]. This instability may switch off at $j \rightarrow 0$ (1). In analogy to the *ve*-dimensional case [107, 104], one could also study turning points of j . If these are absent, pinched black holes would presumably be stable to radial

perturbations.

Other compactified solutions. It would also be interesting to examine the existence of other classes of solutions with a compactified direction. For example in Ref. [108] a supersymmetric rotating black hole in a compactified space-time was found and charged black holes in compactified space-times are considered in Ref. [109]. In another direction, new solutions with Kaluza-Klein boundary conditions for anti-de-Sitter spacetimes have recently been constructed in Refs. [110, 111]. Finally, rotating non-uniform solutions in KK space have been constructed numerically in Ref. [112] (see also Ref. [113]).

Numerical solutions. For both classes of higher-dimensional black holes presented in this lecture, it would be interesting to attempt to further apply numerical techniques in order to construct the new solutions. For example, for multi-black hole configurations on the cylinder this could confirm whether there are multi-black hole solutions for which the temperatures converge when approaching the merger points (as discussed in Ref. [35]). Furthermore, one could try to confirm the existence of the conjectured lumpy black holes (see Sec. 4.3). Similarly, for rotating black holes, numerical construction of the entire black ring phase and of the pinched black hole phase would be very interesting.

Effective field theory techniques. As mentioned in Sec. 2.2, an alternative to the matched expansion is the use of classical effective field theory [44, 45] to obtain the corrected thermodynamics of new solutions in a perturbative expansion. It would be interesting to use this method to go beyond the first order for the solutions discussed in this lecture and apply it to other extended brane-like black holes with or without rotation.

Other black rings. The method used to construct thin black rings in asymptotically flat space can also be used to study thin black rings in external gravitational potentials, yielding e.g. black Saturn or black rings in AdS or dS spacetime.⁷ Similarly, one could study black rings with charges [115, 116] and with dipoles [99]. In this connection we note that the existence of small supersymmetric black rings in $D = 5$ was argued in [17].

More rotation parameters. One may try to extend the analysis to black rings with horizon $S^1 \times S^{n+1}$ with rotation not only along S^1 but also in the S^{n+1} . Rotation in the S^{n+1} will introduce particularly rich dynamics for $n \geq 3$, since it is then possible to have ultra-spinning regimes for this rotation too, leading to pinches of the S^{n+1} and further connections to phases with horizon $S^1 \times S^1 \times S^n$, and so forth.

Black folds. Following the construction in Sec. 5, one can envision many generalizations. In this way one could study the possible existence of more general blackfolds, obtained by taking a black p-brane with horizon topology $R^p \times S^q$ and bending R^p to form some compact manifold. One must then find out under which conditions a curved black p-brane can satisfy the equilibrium equation (50). This method is constructive and uses dynamical information to determine possible horizon geometries. In contrast, conventional

⁷In [114] the existence of supersymmetric black rings in AdS is considered.

approaches based on topological considerations are non-constructive and have only found very weak restrictions in six or more dimensions [118, 119].

Plasma balls and rings. There is also another more indirect approach to higher-dimensional black rings in AdS, using the AdS/CFT correspondence. In Ref. [120] stationary, axially symmetric spinning configurations of plasma in $N = 4$ SYM theory compactified to $d = 3$ on a Scherk-Schwarz circle were studied. On the gravity side, these correspond to large rotating black holes and black rings in the dual Scherk-Schwarz compactified AdS₅ space. Interestingly, the phase diagram of these rotating fluid configurations, even if dual to black holes larger than the AdS radius, reproduces many of the qualitative features of the MP black holes and black rings in five-dimensional flat spacetime. Higher-dimensional generalizations of this setup give predictions for the phases of black holes in Scherk-Schwarz compactified AdS_D with $D > 5$. In this way, evidence was found [120] for rotating black rings and ‘pinched’ black holes in AdS₆, that can be considered the AdS-analogues of the phases conjectured in [36, 30], discussed in Secs. 5 and 6.

Microscopic entropy for three-charge black holes. One could extend the work of Ref. [121, 122] by applying the boost/U-duality map of [11] to the multi-black hole configurations of Ref. [35]. In particular, this would enable to compute the first correction to the finite entropy of the resulting three-charge multi-black hole configurations on a circle. It would be interesting to then try to derive these expressions from a microscopic calculation following the single three-charge black hole case considered in Refs. [121, 123].

Braneworld black holes. The higher dimensional black holes and branes described in this lecture also appear naturally in the discussion of the braneworld model of large extra dimensions [124, 13]. In other braneworld models such as the one proposed by Randall and Sundrum [125, 126] the geometry is warped in the extra direction and the discovery of black hole solutions in this context has proven more difficult. It would be interesting to consider the higher-dimensional black hole solutions considered in this lecture in these contexts.

Acknowledgements

I would like to thank the organizers, especially Lefteris Papantonopoulos, of the Fourth Aegean Summer School on Black Holes (Sept. 17-22, 2007, Mytiline, Island of Lesbos, Greece) for a stimulating and interesting school. I also thank Oscar Dias, Roberto Emparan, Troels Harmark, Rob Myers, Vasilis Niarchos and Maria Jose Rodriguez for collaboration on the work presented here. This work is partially supported by the European Community’s Human Potential Programme under contract MRTN-CT-2004-005104 ‘Constituents, fundamental forces and symmetries of the universe’.

References

- [1] B. Kol, "The phase transition between caged black holes and black strings: A review," *Phys. Rept.* 422 (2006) 119{165, hep-th/0411240.
- [2] R. Emparan and H. S. Reall, "Black rings," *Class. Quant. Grav.* 23 (2006) R169, hep-th/0608012.
- [3] T. Harmark, V. Niarchos, and N. A. Obers, "Instabilities of black strings and branes," *Class. Quant. Grav.* 24 (2007) R1{R90, hep-th/0701022.
- [4] R. Emparan and H. S. Reall, "Black Holes in Higher Dimensions," arXiv:0801.3471 [hep-th].
- [5] A. Strominger and C. Vafa, "Microscopic origin of the Bekenstein-Hawking entropy," *Phys. Lett. B* 379 (1996) 99{104, hep-th/9601029.
- [6] S. D. Mathur, "The fuzzball proposal for black holes: An elementary review," *Fortsch. Phys.* 53 (2005) 793{827, hep-th/0502050.
- [7] S. D. Mathur, "The quantum structure of black holes," *Class. Quant. Grav.* 23 (2006) R115, hep-th/0510180.
- [8] J. M. Maldacena, "The large N limit of superconformal field theories and supergravity," *Adv. Theor. Math. Phys.* 2 (1998) 231{252, hep-th/9711200.
- [9] O. Aharony, S. S. Gubser, J. Maldacena, H. Ooguri, and Y. Oz, "Large N field theories, string theory and gravity," *Phys. Rept.* 323 (2000) 183, hep-th/9905111.
- [10] O. Aharony, J. Marsano, S. Minwalla, and T. Wiseman, "Black hole - black string phase transitions in thermal 1+1 dimensional supersymmetric Yang-Mills theory on a circle," *Class. Quant. Grav.* 21 (2004) 5169{5192, hep-th/0406210.
- [11] T. Harmark and N. A. Obers, "New phases of near-extremal branes on a circle," *JHEP* 09 (2004) 022, hep-th/0407094.
- [12] N. Arkani-Hamed, S. Dimopoulos, and G. R. Dvali, "The hierarchy problem and new dimensions at a millimeter," *Phys. Lett. B* 429 (1998) 263{272, hep-ph/9803315.
- [13] I. Antoniadis, N. Arkani-Hamed, S. Dimopoulos, and G. R. Dvali, "New dimensions at a millimeter to a Fermi and superstrings at a TeV," *Phys. Lett. B* 436 (1998) 257{263, hep-ph/9804398.
- [14] P. Kanti, "Black holes in theories with large extra dimensions: A review," *Int. J. Mod. Phys. A* 19 (2004) 4899{4951, hep-ph/0402168.

- [15] R. C. Myers and M. J. Perry, "Black holes in higher dimensional spacetimes," *Ann. Phys.* 172 (1986) 304.
- [16] R. Emparan and H. S. Reall, "A rotating black ring in five dimensions," *Phys. Rev. Lett.* 88 (2002) 101101, hep-th/0110260.
- [17] H. Elvang and P. Figueras, "Black saturn," *JHEP* 05 (2007) 050, hep-th/0701035.
- [18] H. Elvang, R. Emparan, and P. Figueras, "Phases of five-dimensional black holes," *JHEP* 05 (2007) 056, hep-th/0702111.
- [19] H. Iguchi and T. Mishima, "Black di-ring and infinite nonuniqueness," *Phys. Rev. D* 75 (2007) 064018, hep-th/0701043.
- [20] J. Evslin and C. Krishnan, "The black di-ring: An inverse scattering construction," arXiv:0706.1231 [hep-th].
- [21] A. A. Pomerenansky and R. A. Sen'kov, "Black ring with two angular momenta," hep-th/0612005.
- [22] K. Izumi, "Orthogonal black di-ring solution," arXiv:0712.0902 [hep-th].
- [23] H. Elvang and M. J. Rodriguez, "Bicycling black rings," arXiv:0712.2425 [hep-th].
- [24] R. Emparan and H. S. Reall, "Generalized Weyl solutions," *Phys. Rev. D* 65 (2002) 084025, hep-th/0110258.
- [25] T. Harmark, "Stationary and axisymmetric solutions of higher-dimensional general relativity," *Phys. Rev. D* 70 (2004) 124002, hep-th/0408141.
- [26] V. A. Belinsky and V. E. Zakharov, "Integration of the Einstein equations by the inverse scattering problem technique and the calculation of the exact soliton solutions," *Sov. Phys. JETP* 48 (1978) 985(994).
- [27] V. A. Belinsky and V. E. Zakharov, "Stationary gravitational solitons with axial symmetry," *Sov. Phys. JETP* 50 (1979) 1.
- [28] V. Belinski and E. Verdaguer, "Gravitational solitons," Cambridge, UK: Univ. Pr. (2001) 258 p.
- [29] A. A. Pomerenansky, "Complete integrability of higher-dimensional Einstein equations with additional symmetry, and rotating black holes," *Phys. Rev. D* 73 (2006) 044004, hep-th/0507250.
- [30] R. Emparan, T. Harmark, V. Niarchos, N. A. Obers, and M. J. Rodriguez, "The phase structure of higher-dimensional black rings and black holes," *JHEP* 10 (2007) 110, arXiv:0708.2181 [hep-th].

- [31] T. Harmark, "Small black holes on cylinders," *Phys. Rev. D* 69 (2004) 104015, hep-th/0310259.
- [32] D. Gorbounov and B. Kol, "A dialogue of multipoles: Matched asymptotic expansion for caged black holes," *JHEP* 06 (2004) 053, hep-th/0406002.
- [33] D. Karasik, C. Sahabandu, P. Suranyi, and L. C. R. Wijewardhana, "Analytic approximation to 5 dimensional black holes with one compact dimension," *Phys. Rev. D* 71 (2005) 024024, hep-th/0410078.
- [34] D. Gorbounov and B. Kol, "Matched asymptotic expansion for caged black holes: Regularization of the post-Newtonian order," *Class. Quant. Grav.* 22 (2005) 3935{3960, hep-th/0505009.
- [35] O. J. C. Dias, T. Harmark, R. C. Myers, and N. A. Obers, "Multi-black hole configurations on the cylinder," *Phys. Rev. D* 76 (2007) 104025, arXiv:0706.3645 [hep-th].
- [36] R. Emparan and R. C. Myers, "Instability of ultra-spinning black holes," *JHEP* 09 (2003) 025, hep-th/0308056.
- [37] S. S. Gubser, "On non-uniform black branes," *Class. Quant. Grav.* 19 (2002) 4825{4844, hep-th/0110193.
- [38] T. Wiseman, "Static axisymmetric vacuum solutions and non-uniform black strings," *Class. Quant. Grav.* 20 (2003) 1137{1176, hep-th/0209051.
- [39] E. Sorkin, "A critical dimension in the black-string phase transition," *Phys. Rev. Lett.* 93 (2004) 031601, hep-th/0402216.
- [40] B. Kleihaus, J. Kunz, and E. Radu, "New nonuniform black string solutions," *JHEP* 06 (2006) 016, hep-th/0603119.
- [41] E. Sorkin, "Non-uniform black strings in various dimensions," *Phys. Rev. D* 74 (2006) 104027, gr-qc/0608115.
- [42] B. Kleihaus and J. Kunz, "Interior of nonuniform black strings," arXiv:0710.1726 [hep-th].
- [43] T. Harmark and N. A. Obers, "Black holes on cylinders," *JHEP* 05 (2002) 032, hep-th/0204047.
- [44] Y.-Z. Chu, W. D. Goldberger, and I. Z. Rothstein, "Asymptotics of d-dimensional Kaluza-Klein black holes: Beyond the Newtonian approximation," *JHEP* 03 (2006) 013, hep-th/0602016.

- [45] B. Kol and M. Sorkin, "Classical effective field theory and caged black holes," arXiv:0712.2822 [hep-th].
- [46] E. Sorkin, B. Kol, and T. Piran, "Caged black holes: Black holes in compactified spacetimes. II: 5d numerical implementation," Phys. Rev. D 69 (2004) 064032, hep-th/0310096.
- [47] H. Kudoh and T. Wiseman, "Properties of Kaluza-Klein black holes," Prog. Theor. Phys. 111 (2004) 475{507, hep-th/0310104.
- [48] H. Kudoh and T. Wiseman, "Connecting black holes and black strings," Phys. Rev. Lett. 94 (2005) 161102, hep-th/0409111.
- [49] H. Elvang, T. Harmark, and N. A. Obers, "Sequences of bubbles and holes: New phases of Kaluza-Klein black holes," JHEP 01 (2005) 003, hep-th/0407050.
- [50] T. Harmark and N. A. Obers, "New phase diagram for black holes and strings on cylinders," Class. Quantum Grav. 21 (2004) 1709{1724, hep-th/0309116.
- [51] B. Kol, E. Sorkin, and T. Piran, "Caged black holes: Black holes in compactified spacetimes. I: Theory," Phys. Rev. D 69 (2004) 064031, hep-th/0309190.
- [52] T. Harmark and N. A. Obers, "Phase structure of black holes and strings on cylinders," Nucl. Phys. B 684 (2004) 183{208, hep-th/0309230.
- [53] R. Gregory and R. Laamane, "Black strings and p-branes are unstable," Phys. Rev. Lett. 70 (1993) 2837{2840, hep-th/9301052.
- [54] R. Gregory and R. Laamane, "The instability of charged black strings and p-branes," Nucl. Phys. B 428 (1994) 399{434, hep-th/9404071.
- [55] B. Kol, "Topology change in general relativity and the black-hole black-string transition," hep-th/0206220.
- [56] T. Wiseman, "From black strings to black holes," Class. Quant. Grav. 20 (2003) 1177{1186, hep-th/0211028.
- [57] B. Kol and T. Wiseman, "Evidence that highly non-uniform black strings have a conical waist," Class. Quant. Grav. 20 (2003) 3493{3504, hep-th/0304070.
- [58] B. Kol and E. Sorkin, "On black-brane instability in an arbitrary dimension," Class. Quant. Grav. 21 (2004) 4793{4804, gr-qc/0407058.
- [59] B. Kol and E. Sorkin, "LG (Landau-Ginzburg) in GL (Gregory-Laamane)," Class. Quant. Grav. 23 (2006) 4563{4592, hep-th/0604015.
- [60] W. Israel, "Event horizons in static vacuum spacetimes," Phys. Rev. 164 (1967) 1776{1779.

- [61] B. Carter, "Axisymmetric black hole has only two degrees of freedom," *Phys. Rev. Lett.* 26 (1971) 331{333.
- [62] S.W. Hawking, "Black holes in General Relativity," *Commun. Math. Phys.* 25 (1972) 152{166.
- [63] D.C. Robinson, "Uniqueness of the Kerr black hole," *Phys. Rev. Lett.* 34 (1975) 905{906.
- [64] T. Regge, "Stability of a Schwarzschild singularity," *Phys. Rev.* 108 (1957) 1063{1069.
- [65] F.J. Zerilli, "Gravitational field of a particle falling in a Schwarzschild geometry analyzed in tensor harmonics," *Phys. Rev. D* 2 (1970) 2141{2160.
- [66] S.A. Teukolsky, "Perturbations of a rotating black hole. 1. Fundamental equations for gravitational electromagnetic, and neutrino field perturbations," *Astrophys. J.* 185 (1973) 635{647.
- [67] H. Kodama, "Perturbations and stability of higher-dimensional black holes," arXiv:0712.2703 [hep-th].
- [68] F.R. Tangherlini, "Schwarzschild field in n dimensions and the dimensionality of space problem," *Nuovo Cimento* 27 (1963) 636.
- [69] G.W. Gibbons, D. Ida, and T. Shiromizu, "Uniqueness and non-uniqueness of static vacuum black holes in higher dimensions," *Prog. Theor. Phys. Suppl.* 148 (2003) 284{290, gr-qc/0203004.
- [70] G.W. Gibbons, D. Ida, and T. Shiromizu, "Uniqueness and non-uniqueness of static black holes in higher dimensions," *Phys. Rev. Lett.* 89 (2002) 041101, hep-th/0206049.
- [71] H. Kodama and A. Ishibashi, "A master equation for gravitational perturbations of maximally symmetric black holes in higher dimensions," *Prog. Theor. Phys.* 110 (2003) 701{722, hep-th/0305147.
- [72] A. Ishibashi and H. Kodama, "Stability of higher-dimensional Schwarzschild black holes," *Prog. Theor. Phys.* 110 (2003) 901{919, hep-th/0305185.
- [73] H. Kodama and A. Ishibashi, "Master equations for perturbations of generalized static black holes with charge in higher dimensions," *Prog. Theor. Phys.* 111 (2004) 29{73, hep-th/0308128.
- [74] S. Hollands, A. Ishibashi, and R.M. Wald, "A higher dimensional stationary rotating black hole must be axisymmetric," *Commun. Math. Phys.* 271 (2007) 699{722, gr-qc/0605106.

- [91] V. Cardoso and L. Gualtieri, "Equilibrium configurations of fluids and their stability in higher dimensions," *Class. Quant. Grav.* 23 (2006) 7151{7198, hep-th/0610004.
- [92] R. Gregory and R. Laamane, "Hypercylindrical black holes," *Phys. Rev. D* 37 (1988) 305.
- [93] R. C. Myers, "Higher dimensional black holes in compactified spaces," *Phys. Rev. D* 35 (1987) 455.
- [94] A. R. Bogojevic and L. Perivolaropoulos, "Black holes in a periodic universe," *Mod. Phys. Lett. A* 6 (1991) 369{376.
- [95] D. Krotkin and H. Nicolai, "A periodic analog of the Schwarzschild solution," gr-qc/9403029.
- [96] A. V. Frolov and V. P. Frolov, "Black holes in a compactified spacetime," *Phys. Rev. D* 67 (2003) 124025, hep-th/0302085.
- [97] P.-J. De Smet, "Black holes on cylinders are not algebraically special," *Class. Quant. Grav.* 19 (2002) 4877{4896, hep-th/0206106.
- [98] G. T. Horowitz, "Playing with black strings," hep-th/0205069.
- [99] R. Emparan, "Rotating circular strings, and infinite non-uniqueness of black rings," *JHEP* 03 (2004) 064, hep-th/0402149.
- [100] V. Cardoso, O. J. C. Dias, and L. Gualtieri, "The return of the membrane paradigm? Black holes and strings in the water tap," arXiv:0705.2777 [hep-th].
- [101] T. Harmark and P. Olesen, "On the structure of stationary and axisymmetric metrics," *Phys. Rev. D* 72 (2005) 124017, hep-th/0508208.
- [102] H. Elvang and R. Emparan, "Black rings, supertubes, and a stringy resolution of black hole non-uniqueness," *JHEP* 11 (2003) 035, hep-th/0310008.
- [103] J. L. Horvdebo and R. C. Myers, "Black rings, boosted strings and Gregory-Laamane," *Phys. Rev. D* 73 (2006) 084013, hep-th/0601079.
- [104] H. Elvang, R. Emparan, and A. Virmani, "Dynamics and stability of black rings," *JHEP* 12 (2006) 074, hep-th/0608076.
- [105] B. Carter, "Essentials of classical brane dynamics," *Int. J. Theor. Phys.* 40 (2001) 2099{2130, gr-qc/0012036.
- [106] D. Kastor, S. Ray, and J. Traschen, "The first law for boosted Kaluza-Klein black holes," *JHEP* 06 (2007) 026, arXiv:0704.0729 [hep-th].

- [107] G. Arcioni and E. Lozano-Tellechea, "Stability and critical phenomena of black holes and black rings," *Phys. Rev. D* 72 (2005) 104021, hep-th/0412118.
- [108] K.-i. Maeda, N. Ohta, and M. Tanabe, "A supersymmetric rotating black hole in a compactified spacetime," *Phys. Rev. D* 74 (2006) 104002, hep-th/0607084.
- [109] M. Karlovini and R. von Unge, "Charged black holes in compactified spacetimes," *Phys. Rev. D* 72 (2005) 104013, gr-qc/0506073.
- [110] K. Copsey and G. T. Horowitz, "Gravity dual of gauge theory on $S^2 \times S^1 \times R$," *JHEP* 06 (2006) 021, hep-th/0602003.
- [111] R. B. Mann, E. Radu, and C. Stelea, "Black string solutions with negative cosmological constant," *JHEP* 09 (2006) 073, hep-th/0604205.
- [112] B. Kleihaus, J. Kunz, and E. Radu, "Rotating nonuniform black string solutions," *JHEP* 05 (2007) 058, hep-th/0702053.
- [113] B. Kleihaus, J. Kunz, and F. Navarro-Lerida, "Rotating black holes in higher dimensions," arXiv:0710.2291 [hep-th].
- [114] H. K. Kunduri, J. Lucietti, and H. S. Reall, "Do supersymmetric anti-de Sitter black rings exist?," *JHEP* 02 (2007) 026, hep-th/0611351.
- [115] H. Elvang, "A charged rotating black ring," hep-th/0305247.
- [116] H. Elvang, R. Emparan, D. Mateos, and H. S. Reall, "A supersymmetric black ring," *Phys. Rev. Lett.* 93 (2004) 211302, hep-th/0407065.
- [117] A. Dabholkar, N. Iizuka, A. Iqbal, A. Sen, and M. Shigemori, "Spinning strings as small black rings," *JHEP* 04 (2007) 017, hep-th/0611166.
- [118] C. Helfgott, Y. Oz, and Y. Yanay, "On the topology of black hole event horizons in higher dimensions," *JHEP* 02 (2006) 025, hep-th/0509013.
- [119] G. J. Galloway and R. Schoen, "A generalization of Hawking's black hole topology theorem to higher dimensions," *Commun. Math. Phys.* 266 (2006) 571-576, gr-qc/0509107.
- [120] S. Lahiri and S. M. Inwalla, "Plasmaring as dual black rings," arXiv:0705.3404 [hep-th].
- [121] T. Harmark, K. R. Kristjansson, N. A. Obers, and P. B. Ronne, "Three-charge black holes on a circle," *JHEP* 01 (2007) 023, hep-th/0606246.
- [122] T. Harmark, K. R. Kristjansson, N. A. Obers, and P. B. Ronne, "Entropy of three-charge black holes on a circle," *Fortsch. Phys.* 55 (2007) 748-753, hep-th/0701070.

- [123] B. D. Chowdhury, S. Giusto, and S. D. Mathur, "A microscopic model for the black hole - black string phase transition," Nucl. Phys. B 762 (2007) 301-343, hep-th/0610069.
- [124] N. Arkani-Hamed, S. Dimopoulos, and G. R. Dvali, "The hierarchy problem and new dimensions at a millimeter," Phys. Lett. B 429 (1998) 263-272, hep-ph/9803315.
- [125] L. Randall and R. Sundrum, "A large mass hierarchy from a small extra dimension," Phys. Rev. Lett. 83 (1999) 3370-3373, hep-ph/9905221.
- [126] L. Randall and R. Sundrum, "An alternative to compactification," Phys. Rev. Lett. 83 (1999) 4690-4693, hep-th/9906064.